JOTCS A
Journal of the Turkish Chemical Society
Section: A
Chemistry
TURKISH CHEMICAL SOCIETY

Molecular docking studies and biological activities of benzenesulfonamide-based thiourea and thiazolidinone derivatives targeting cholinesterases, α-glucosidase, and α-amylase enzymes

Mehtap Tugrak Sakarya[1*], Halise Inci Gul[2], Cem Yamali[3], Parham Taslimi[4], and Tugba Taskin Tok[5,6]

[1]Gaziosmanpasa University, Department of Pharmaceutical Chemistry, Tokat, Turkey.
[2]Ataturk University, Department of Pharmaceutical Chemistry, Erzurum, Turkey.
[3]Cukurova University, Department of Basic Pharmaceutical Sciences, Adana, Turkey.
[4]Bartin University, Department of Biotechnology, Faculty of Science, Bartin, Turkey.
[5]Gaziantep University, Department of Chemistry, Gaziantep, Turkey.
[6]Gaziantep University, Department of Bioinformatics and Computational Biology, Gaziantep, Turkey.

Abstract: Alzheimer's disease (AD) and diabetes mellitus (DM) are related to abnormal changes in enzyme activity. While acetylcholinesterase (AChE) and butyrylcholinesterase (BChE) are the primary targets in the treatment of Alzheimer's disease (AD), α-glucosidase (α-Gly) and α-amylase (α-Amy) enzymes are known for diabetes mellitus (DM). Here, benzenesulfonamide-based thiourea and thiazolidinone derivatives such as AChE, BChE, α-Gly, and α-Amy inhibitors were reported. The results revealed that compounds **1d** and **2c** showed promising AChE and BChE inhibition effects. Compound **2a** was the most potent inhibitor against α-glycosidase and α-amylase, respectively. Molecular docking studies indicated that the lead compounds' binding energy values and molecular interactions were better than that of tacrine and acarbose. The most bioactive compounds may be considered potent leads for further studies.

Keywords: Thiazolidinone, Benzamide, 'Alzheimer's disease, Diabetes Mellitus, Molecular Docking, Synthesis

Submitted: May 8, 2022. **Accepted:** October 26, 2022.

Cite this: Tugrak Sakarya M, Gul HI, Yamali C, Taslimi P, Taskin Tok T. Molecular docking studies and biological activities of benzenesulfonamide-based thiourea and thiazolidinone derivatives targeting cholinesterases, α-glucosidase, and α-amylase enzymes. JOTCSA. 2023;10(2):385-424

DOI: https://doi.org/10.18596/jotcsa.1111172

***Corresponding author's E-mail:** mehtaptugrak@hotmail.com

1. INTRODUCTION

Alzheimer's disease (AD) is a neurodegenerative disease in the elderly worldwide characterized by degeneration of cholinergic neurons in the brain. Decreased cholinergic signal transmission leads to some cognitive dysfunctions during the progression of the disease (1). Based on the cholinergic approach, acetylcholinesterase (AChE) and butyrylcholinesterase (BChE) enzymes are considered therapeutic targets of AD (2). Presently, the most used anti-AD drugs in the clinic are AChE inhibitors such as donepezil, rivastigmine, and galantamine (3, 4) (Figure 1). AChE inhibitors interact mainly on the active catalytic site (CAS) below AChE (3). This situation may relieve the symptoms of patients with mild to moderate. However, recent studies have demonstrated that the peripheral active site (PAS) is closely related to the neurotoxic cascade of AD. Therefore, dual interactions with CAS and PAS sites lead to favorable AChE inhibitory activity (3).

Diabetes has become a severe health problem globally since 425 million people have diabetes, and it is expected to reach approximately 700 million by 2045 (5). Type 2 diabetes (T2D, not insulin-dependent) affects 85-90% of the entire diabetic population (6). The most effective way to prevent T2D is to inhibit starch hydrolysis from slowing glucose absorption in starchy foods. Alpha (α)-amylase and alpha (α)-glucosidase is two main

hydrolytic enzymes that have a role in this process (7, 8). Acarbose is the oral glucose-lowering drug used in the treatment that delays glucose absorption. Despite acarbose being a popular glucose-lowering drug, it causes severe side effects such as liver disorders, diarrhea, flatulence, and abdominal cramps (9, 10). In addition, glibenclamide, gliquidone, rosiglitazone, and pioglitazone are widely used for the initial treatment of T2D (Figure 1) (11-14). Using these hypoglycemic agents may lead to gastrointestinal reactions, skin allergies, and hypoglycemia (11, 12). Therefore, discovering novel and effective drug candidates for treating diabetes without causing side effects is needed.

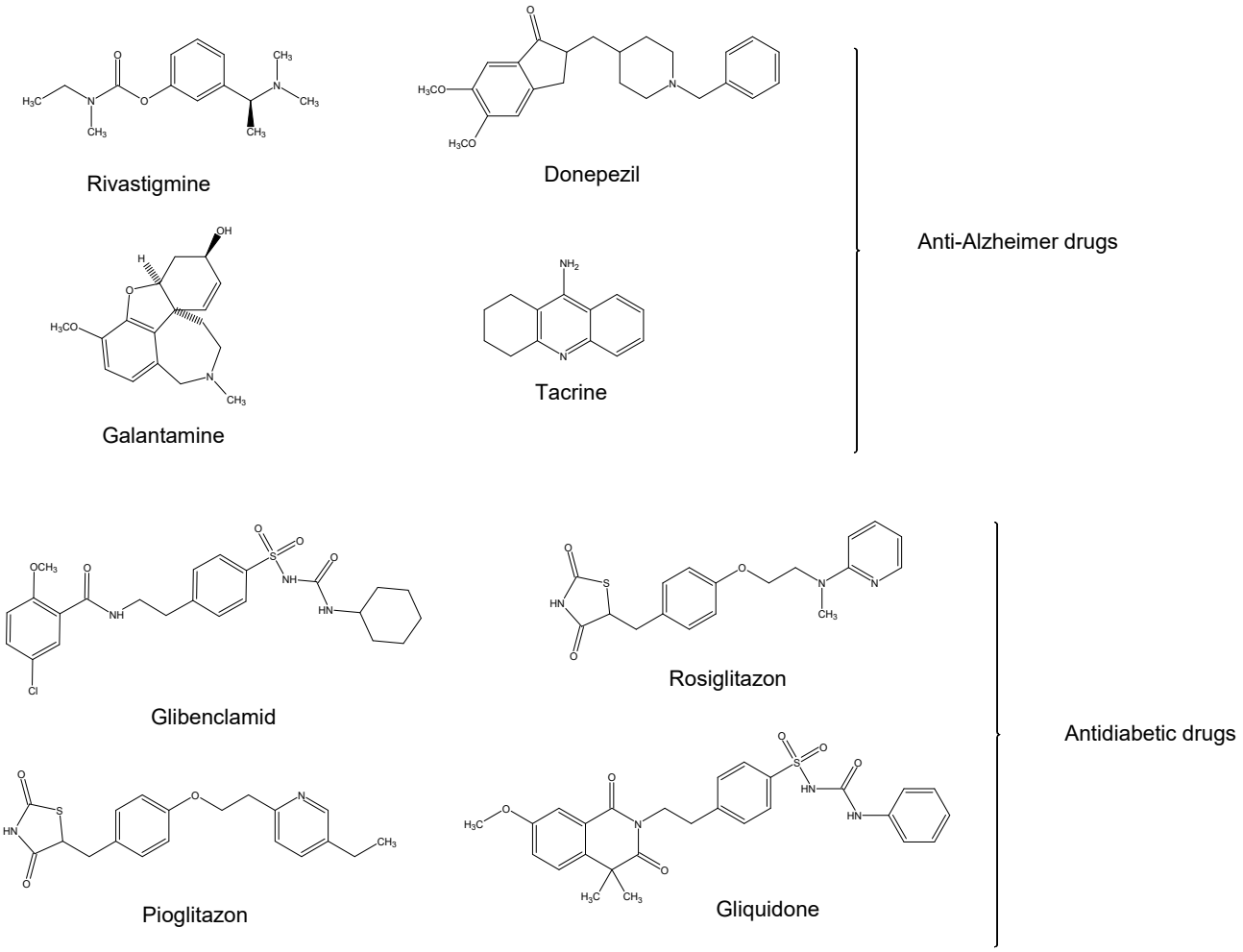

Figure 1: Commonly used drugs in Alzheimer's disease (up) and diabetes mellitus (down)

Clinical studies have shown that diabetes increases the risk of AD. Diabetes patients have 1.5-2 times more risk of having AD than healthy people (15-17). Clinical studies point out that both diseases have common pathological mechanisms to exacerbate neurodegeneration in the brain. Relationships between diabetes and AD have been studied in detail, and studies have reported that hyperglycemia, vascular damage, hypoglycemia, and insulin resistance are among the most likely pathophysiological causes (18-20). In addition, in both diseases, oxidative stress, vascular dysfunctions, amyloidogenesis, and disorders in glucose and fatty acid metabolism occur, and oxidatively modified proteins accumulate (21, 22). In addition, neuropathological markers of AD such as APP, Aβ, and phosphatase increased in using both T1D and T2D model transgenic rats; on the other hand, intracellular components in the insulin receptor pathway such as phospho AKT (protein kinase B), phospho glycogen synthase kinase-3β (GSK3β) have been shown to decrease (20). Hypothetical models are suggested that diabetes mellitus induces AD pathology and cognitive dysfunction (23).

Thiazolidinone derivatives show a wide range of biological activities such as anti-Alzheimer, antidiabetic, antibacterial, anticancer, and antitubercular (24-26). Recently, the effect of thiazolidinone analogs as a muscarinic receptor 1 (M1) agonist in Alzheimer's dementia models were reported. Based on the results obtained, derivative **1** (Figure 2), which has the diphenylamine moiety attached to the nitrogen of the thiazolidinone, showed a significant affinity for M1 receptor binding (1). In another study, thiazole-based compounds were reported as AChE inhibitors at the nanomolar level. According to the study, compounds **2** (Figure 2) and **3** (Figure 2) could be considered potent AChE inhibitors with IC_{50} values of 103.24 nM and 108.94

nM. The thiazole core was also reported as an important moiety having promising interactions with the active site of AChE (27).

Primary and secondary sulfonamide derivatives are valuable compounds with different biological activities in drug discovery. Markowicz-Piaseckaa et al. (28) reported the effects of sulfonamide derivatives of metformin on both AChE, BuChE activity, and β-amyloid aggregation. Compound **4** (Figure 2) inhibited AChE in a mixed-type manner at micromolar concentrations (IC_{50}=212.5 ± 48.3 μmol/L). Compound **4** also inhibited Aβ aggregation at 200 μmol/L (28). Our studies also indicated that sulfonamide-based compounds could be considered potent and selective cholinesterase inhibitors. In our previous study, 4-(3-(difluorophenyl)-5-(dimethoxyphenyl)-4,5-dihydropyrazol-1-yl) benzenesulfonamides (**5-12**) (Figure 2) inhibited AChE enzyme in the range of 3.28 ± 1.47 – 9.77 ± 1.86 nM (29). AChE inhibition and molecular docking studies showed that pyrazole-based benzenesulfonamide derivative **13** (Figure 2) also showed a good inhibitory effect with a Ki value of 22.713 ± 10.33 nM (30).

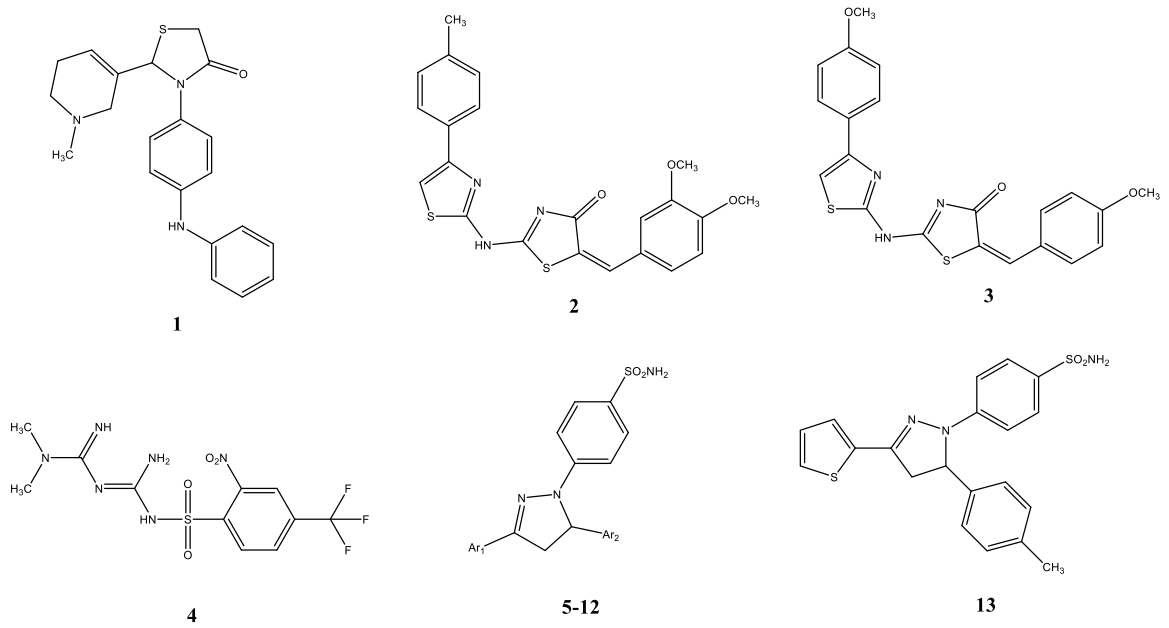

Figure 2: Structures of the compounds **1-13**

Based on the reports, we synthesized thiazolidinone derivatives (Figure 3) to evaluate their *in vitro* biological effects on AChE, BChE, α-Amy, and α-Gly enzymes. Moreover, docking studies were carried out on the most potent compounds to predict the binding poses to the enzymes studied.

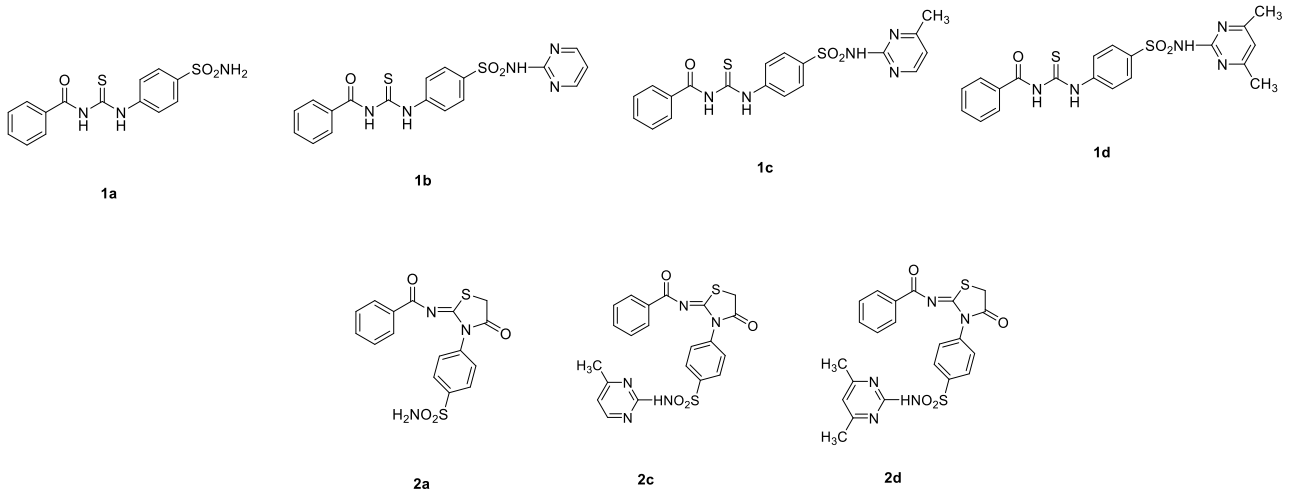

Figure 3: Chemical structures of the thiazolidinone derivatives **1a-d, 2a, 2c, 2d**

2. EXPERIMENTAL SECTION

2.1. Chemistry

^{1}H NMR (400 MHz) and ^{13}C NMR (100 MHz) spectra in DMSO-d_6 (Merck) were taken using a Varian Mercury Plus spectrometer, Varian Inc., Palo Alto, California, US A liquid chromatography ion trap-time of flight tandem mass spectrometer (Shimadzu, Kyoto, Japan) was used to get Mass spectra (HRMS) for the compounds. Data analysis was done by 'Shimadzu's LCMS Solution software. 9100/IA9100 instrument (Bibby Scientific Limited, Staffordshire, UK) was used to determine melting points. Reactions were monitored by Thin Layer Chromatography (TLC) using silica gel HF254 (Merck Art 5715).

2.2. General synthesis procedure of 1a-d, Figure 4

The thiourea substituted derivatives **1a-d** used as a starting compound were synthesized previously, and all chemistry details were given in the literature (31).

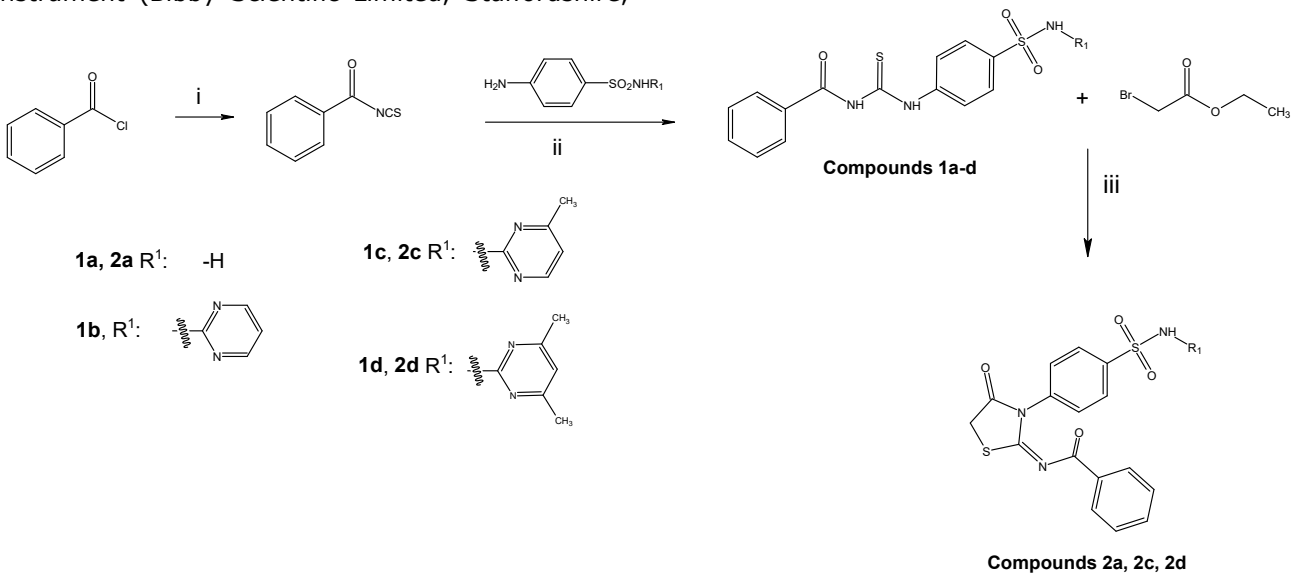

Reaction conditions: (i) KSCN, acetone, reflux, 1.5 hours; (ii) acetone, reflux, 4-8 hours; (iii) ethyl bromoacetate, EtOH, reflux, 15-24 hours

Figure 4: Synthesis of the compounds **1a-d, 2a, 2c, 2d.**

*N-[(4-Sulfamoylphenyl)carbamothioyl]benzamide (**1a**)*

White-colored solid, mp: 234-236°C, yield 86 %. ^{1}H NMR (DMSO-d_6, ppm, 400 MHz), δ 12.72 (s, 1H, NH), 11.70 (s, 1H, NH), 8.00-7.98 (m, 2H, Ar-H), 7.93-7.85 (m, 4H, Ar-H), 7.70-7.66 (m, 1H, Ar-H), 7.57-7.53 (m, 2H, Ar-H), 7.41 (s, 2H, NH_2); ^{13}C NMR (DMSO-d_6, ppm, 100 MHz) δ 179.9 (C=S), 168.7 (C=O), 141.8, 141.4, 133.7, 132.5, 129.2, 128.9, 126.7, 124.8; HRMS (ESI-MS) $C_{14}H_{13}N_3O_3S_2$, Calculated $[M-H]^-$: 334.0326; Found $[M-H]^-$: 334.0330.

*N-{[4-(N'-(Pyrimidin-2-yl)sulfamoyl)phenyl]carbamothioyl}benzamide (**1b**)*

Light cream-colored solid, mp: 250-252°C, yield 88 %. ^{1}H NMR (DMSO-d_6, ppm, 400 MHz), δ 12.75 (s, 1H, NH), 11.70 (s, 1H, NH), 8.54-8.52 (m, 2H, Ar-H), 8.03-7.97 (m, 7H, Ar-H, NH), 7.69-7.65 (m, 1H, Ar-H), 7.56-7.52 (m, 2H, Ar-H), 7.08-7.05 (m, 1H, Ar-H); ^{13}C NMR (DMSO-d_6, ppm, 100 MHz) δ 179.7 (C=S), 168.6 (C=O), 158.9, 157.3, 142.3, 137.8, 133.7, 132.5, 129.2, 128.9, 128.7, 124.3, 116.3; HRMS (ESI-MS) $C_{18}H_{15}N_5O_3S_2$, Calculated $[M+Na]^+$: 436.0509; Found $[M+Na]^+$: 436.0502.

*N-{[4-(N'-(4-Methylpyrimidin-2-yl)sulfamoyl)phenyl]carbamothioyl}benzamide (**1c**)*

Light white-colored solid, mp: 231-232°C, yield 80 %. ^{1}H NMR (DMSO-d_6, ppm, 400 MHz), δ 12.75 (s, 1H, NH), 11.69 (s, 1H, NH), 8.35-8.33 (m, 1H, Ar-H), 8.03-7.94 (m, 7H, Ar-H, NH), 7.68-7.65 (m, 1H, Ar-H), 7.56-7.53 (m, 2H, Ar-H), 6.92-6.91 (m, 1H, Ar-H), 2.33 (s, 3H, CH_3); ^{13}C NMR (DMSO-d_6, ppm, 100 MHz) δ 179.7 (C=S), 168.6 (C=O), 158.7, 157.2, 156.9, 142.1, 138.0, 133.7, 132.5, 129.2, 128.9, 124.1, 23.7; HRMS (ESI-MS) $C_{19}H_{17}N_5O_3S_2$, Calculated $[M+H]^+$: 428.0846; Found $[M+H]^+$: 428.0834.

*N-{[4-(N'-(4,6-Dimethylpyrimidin-2-yl)sulfamoyl)phenyl]carbamothioyl}benzamide (**1d**)*

White-colored solid, mp: 216-218°C, yield 84 %. ^{1}H NMR (DMSO-d_6, ppm, 400 MHz), δ 12.74 (s, 1H, NH), 11.69 (s, 1H, NH), 8.03-7.92 (m, 7H, Ar-H), 7.68-7.64 (m, 1H, Ar-H), 7.56-7.52 (m, 2H, Ar-H), 6.76 (s, 1H, NH), 2.26 (s, 6H, CH_3); ^{13}C NMR (DMSO-d_6, ppm, 100 MHz) δ 179.2 (C=S), 168.1 (C=O), 158.9, 157.2, 156.0, 142.3, 141.4, 133.2, 132.0, 128.69, 128.66, 128.4, 123.4, 22.7; HRMS (ESI-MS) $C_{20}H_{19}N_5O_3S_2$, Calculated $[M+H]^+$: 442.1002; Found $[M+H]^+$: 442.1006.

2.3. General procedure for the synthesis of iminothiazolidinone-sulfonamide hybrids 2a, 2c, 2d, Figure 4

To a stirred solution of thiourea substituted derivatives (**1a-d**) (0.5 mmol) in ethanol (10 mL) were added the ethyl bromoacetate (0.05 mL, 0.5 mmol) and sodium acetate (0.09 g, 1 mmol). The

reaction mixture was refluxed for 15–24 h, and the progress of the reaction was monitored by TLC. On completion, the precipitates formed were filtered and recrystallized from ethanol to afford the products (**2a**, **2c**, **2d**).

*N-(4-oxo-3-(4-sulfamoylphenyl)thiazolidin-2-ylidene)benzamide (**2a**)*

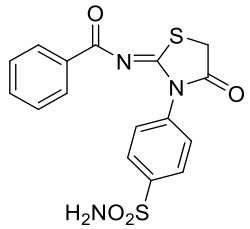

Light white-colored solid, mp: 269-271°C, yield 70 %. ^{1}H NMR (DMSO-d_6, ppm, 400 MHz), δ 8.09 (d, 2H, Ar-H, *J*= 8.5 Hz), 7.84 (d, 2H, Ar-H, *J*= 8.3 Hz), 7.70–7.20 (m, 5H, Ar-H), 6.65 (s, 2H, SO_2NH_2), 4.20 (s, 2H, thiazolidinone); ^{13}C NMR (DMSO-d_6, ppm, 100 MHz) δ175.3 (C=O), 174.0 (C=O), 173.3 (C=N),144.2, 143.3, 138.0, 134.2, 132.3, 129.3, 128.0, 126.2, 33.8; HRMS (ESI-MS) $C_{16}H_{13}N_3O_4S_2$, Calculated $[M+H]^+$: 376.0347; Found $[M+H]^+$: 376.04215.

*N-{3-[4-(N-(4-methylpyrimidin-2-yl)sulfamoyl)phenyl]-4-oxothiazolidin-2-ylidene}benzamide (**2c**)*

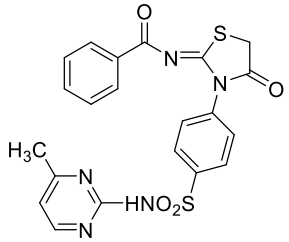

Cream-colored solid, mp: 261-262°C, yield 60 %. ^{1}H NMR (DMSO-d_6, ppm, 400 MHz), δ 8.34 (d, 1H, Ar-H, *J*= 5.1 Hz), 8.15 (d, 2H, Ar-H, *J*= 8.4 Hz), 7.82-7.77 (m, 2H, Ar-H), 7.64 (d, 2H, Ar-H, *J*= 8.4 Hz), 7.57-7.53 (m, 2H, Ar-H), 7.37-7.34 (m, 2H, Ar-H), 6.91 (s, 1H, SO_2NH), 4.14 (s, 2H, thiazolidinone), 2.28 (s, 3H, CH_3); ^{13}C NMR (DMSO-d_6, ppm, 100 MHz) δ 176.7 (C=O), 174.6 (C=O), 173.4 (C=N), 157.9, 157.2, 141.9, 139.1, 135.5, 134.0, 129.9, 129.3, 129.2, 129.1, 114.9, 34.3, 23.8; HRMS (ESI-MS) $C_{21}H_{18}N_5O_4S_2$, Calculated $[M+H]^+$: 468.0722; Found $[M+H]^+$: 468.0777.

*N-{3-[4-(N-(4,6-dimethylpyrimidin-2-yl)sulfamoyl)phenyl]-4-oxothiazolidin-2-ylidene}benzamide (**2d**)*

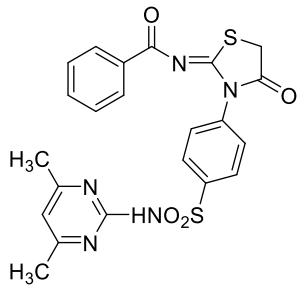

Cream-colored solid, mp: 259-260°C, yield 65 %. ^{1}H NMR (DMSO-d_6, ppm, 400 MHz), δ 8.14 (d, 2H, Ar-H, *J*= 8.4 Hz), 7.79 (d, 2H, Ar-H, *J*= 8.1 Hz), 7.64-7.53 (m, 4H, Ar-H), 7.37-7.34 (m, 2H, Ar-H), 6.75 (s, 1H, SO_2NH), 4.14 (s, 2H, thiazolidinone), 2.23 (s, 6H, CH_3); ^{13}C NMR (DMSO-d_6, ppm, 100 MHz) δ 176.8 (C=O), 174.6 (C=O),173.4 (C=N),156.6, 142.3, 138.8, 135.5, 133.9, 129.8, 129.3, 129.2, 129.1, 34.3, 23.3; HRMS (ESI-MS) $C_{22}H_{19}N_5O_4S_2$, Calculated $[M+H]^+$: 482.0878; Found $[M+H]^+$: 482.09463.

2.4. Pharmacological/biological assays

2.4.1. Acetylcholinesterase and Butyrylcholinesterase inhibition studies

The inhibition effects of the compounds on AChE and BChE enzymes, which were obtained from Electrophorus electricus and equine serum, were performed according to literature (32, 33). Also, acetylthiocholineiodide (AChI) / butyrylthiocholine iodide (BChI) and 5,5′-dithiobis(2-nitrobenzoicacid) (DTNB)were used as substrates for cholinergic reactions (34). Briefly, 0.1 mL of Tris/HCl buffer (pH 8.0, 1.0 M) and different volumes of the compounds solutions. Then, 50 µL of AChE/BChE (5.32×103EU) was transferred to the solutions and incubated for 15 min at room temperature. After this short incubation period, 50 µL of DTNB (0.5 mM) was added, and the reaction started with the addition of 50 µL of AChI/BChI (10 mM). The formation of yellow-colored 5-thio-2-nitrobenzoate anion spectrophotometrically measured the enzymatic hydrolysis as the result of the reaction of DTNB with thiocholine at a wavelength of 412 nm. Also, one AChE unit is the quantity of AChE, which hydrolyses 1.0 mol of AChI to choline(Ch) and acetate per minute at pH 8.0 at 37°C. Similarly, one BChE unit is the quantity of BChE, which hydrolyze s1.0 mol of BChI to Ch and butyrate per min at pH 8.0 at 37°C (35).

2.4.2. α-Glycosidase inhibition studies

α-Glycosidase inhibition effect of the compounds was made according to the method of Tao et al. (36). *p*-Nitrophenyl-D-glucopyranoside (p-NPG) was used as substrate. First, 75 µL of phosphate buffer solution (5 mM, pH 7.4) was added to 20 µL of *α*-glycosidase solution (0.15EU/mL), which was prepared in phosphate buffer (pH 7.4, 5 mM) and 5 µLof different concentrations of the compounds. Then, it was preincubated at 35°C for 10 min before adding *p*-NPG to initiate the reaction. Also, 20 µL of *p*-NPG was transferred in phosphate buffer (pH 7.4, 5 mM) after a short incubation period at 35°C. The absorbances were measured at 405 nm. One *α*-glycosidase unit is the quantity of enzyme that catalyzes the hydrolysis of 1.0 mol *p*-NPG per minute at pH 7.4 (37).

2.4.3. α-Amylase inhibition studies

α-Amylase inhibitory effects of the compounds were realized according to the procedure of Xiao (38) using starch as substrate. For starch preparation, 0.4 M starch mixture was prepared in 80 mL NaOH solution at 80°C for 30 min. Then, 35 µL of starch solution, 35 µL of phosphate buffer (pH 6.9), and 10 µL of different concentrations of the compounds were mixed and incubated at 35°C for 25 min. Lastly, 20

µL of the *α*-amylase solution was added to the final mixture and reincubated for 25 min. The reactions were finished by adding 50 µL of HCl (0.1 M) to each tube. The absorbance was measured at 580 nm. One *α*-amylase unit is defined as the quantity of *α*-amylase required to release 1 µmol of reducing sugar estimated as glucose per min (pH 6.9, 40°C) (37).

2.4.4. Molecular docking study

The compounds (**1a-1d** and **2a, 2c, 2d**) as ligands were sketched and done geometry and frequency optimization at DFT/B3LYP/6-31G* level of Gaussian 09 (39) Figure 5. The X-ray crystal structures of the first three chosen enzymes were uploaded from the Protein Data Bank (PDB as follows: 4EY6 for acetylcholinesterase (AChE), 1P0I for butyrylcholinesterase (BChE) and 1DHK for alpha Amylase (α-Amy) (40). In addition, the potential patterns of the first three enzymes were examined, and the findings in Figures S1-S3 are summarized in the supplementary file. In our study, in vitro studies were conducted against the alpha-glucosidase enzyme from Saccharomyces cerevisiae. Since the 3D structure of the glucosidase enzyme (Saccharomyces cerevisiae a-glucosidase, maltase, EC 3.2.1.20) is not available, within the scope of molecular docking study, Sequence alignment and homology modeling for the relevant species target were performed using Discovery Studio (DS) 3.5 software (41). The homology model for S. cerevisiae α-glucosidase was constructed using the crystal structure of α-D-glucose-linked isomaltase from S. cerevisiae (PDB ID: 3AJ7 and 3A4A), which shares 71.9% identical and 87.2% identical sequence with α-glucosidase. Figure 6 shows the Ramachandran plot with 96.36% of the residue in the most preferred region, 0.17% in the outside area, and 0.58% in the rotamer disallowed regions. Analysis of the Ramachandran plot further strengthens the quality of the S. cerevisiae alpha glucosidase homology model. Therefore, a validated and analyzed homology model was used for the docking study, as given in Figure S4. Furthermore, the molecular docking interactions of the model structure and control compound acarbose created in the study were compared with the existing data in the literature and verified, Figure S5 (42) in supplementary data.

The missing atoms in the respective structures were added, and partial charges were assigned by Discovery Studio (DS) 3.5 (43). Finally, all targets were minimized with CHARMM "55" forcefield. The binding spaces were defined and edited by the binding site tools in DS 3.5 for all the targets in this work. The docking processes were performed by AutoDock Vina (44). The number of modes (poses) was set to 200, and those that displayed the lowest binding energy were chosen for further analysis. All schematic binding interactions were demonstrated with the aid of DS 3.5 (43). Besides these, positive compounds, Tacrine (TAC) for AChE and BChE enzymes, and Acarbose (ACR) for alpha-amylase and alpha-glucosidase were compared and discussed with new compounds.

3. RESULTS AND DISCUSSION

3.1. Chemistry

The compounds **2a, 2c, and 2d** reported were synthesized according to the method outlined in Figure 4. The thiourea-substituted intermediates used were synthesized according to the procedure previously reported by our group (Figure 4) (31). All compounds were characterized and confirmed by ^{1}H NMR, ^{13}C NMR, and HRMS spectral methods (31). Sulfanilamide-based thiourea compounds (1a-d, 1 mmol) were dissolved in ethanol to obtain target compounds. Then, ethyl bromoacetate (1 mmol) and sodium acetate (2 mmol) were added, respectively, and the reaction mixture was refluxed. The reactions were completed in 15-24 h with yields ranging from 60 to 70%. Compounds **2c** and **2d**, which are among the final compounds, were initially reported in the present study (Figure 4). In ^{1}H NMR spectra for the representative compound **2c**, the characteristic methylene protons of the thiazolidinone ring were seen as a singlet at δ 4.14 ppm, and the signals for the -NH- proton were seen at δ 6.91 ppm. In ^{13}C NMR spectra, aromatic and aliphatic peaks of the compounds were at the expected areas. Further HRMS data confirmed the compound **2c** with the values of calculated $[M+H]^+$: 468.0722 and found $[M+H]^+$: 468.0777.

3.2. Bioactivity results

AChE enzyme inactivates the acetylcholine in synaptic spaces by breaking it down into acetate and choline. If acetylcholine in synaptic spaces is inactivated too much, nerve conduction is interrupted, and AD is seen. Anti-cholinesterase drugs, which are utilized in AD therapy, are reversible protein inhibitor compounds (45). They are utilized to postpone the onset of symptoms associated with patient lifestyles like rationale judgment, memory, ability to speak and think, and other thought processes. Selective BChE inhibition is also potentially advantageous for the therapy of AD. It circumvents the classical cholinergic toxicity, a widespread side impact of these inhibitors (46).

ChE inhibition assays of the compounds were investigated according to 'Ellman's method (32). Compounds showed promising inhibitory activities with K_I values ranging between 41.56±6.34 to 88.21±8.32 nM for AChE and 92.18±10.25 to 419.46±58.12 nM for BChE (Table 1). Tacrine, which was the first drug for palliative treatment of AD, had IC_{50} - K_I values of 244.94 nM - 201.85±22.54 nM (AChE) and 216.40 nM - 187.32±34.77 nM (BChE), respectively. Compounds **1d** and **2c** were the most effective ChE inhibitors, with K_I values of 41.56±6.34 and 92.18±10.25 nM against AChE and BChE, respectively. The order of K_I inhibitory activities of the compounds against AChE was **1d** < **2c** < **2d** < **1a** < **2a** < **1c** < **1b**. Moreover, this order was **2c** < **1c** < **1b** < **1a** < **1d** < **2a** < **2d** against BChE. Based on the IC_{50} values, compounds had IC_{50} in the 33.27-93.85 nM range and 105.91-412.52 nM towards AChE and BChE, respectively. The compounds were more favorable AChE inhibitors with lower K_I values

than BChE, so compounds could be considered selective AChE inhibitors.

The American Diabetes Association and the European Diabetes Research Association recommend using α-amylase and α-glycosidase inhibitors as potential first-line agents or in combination with other antihyperglycemic drugs. α-Amylases are the main target in the treatment of diabetes because inhibition of these enzymes delays glucose absorption. Delaying carbohydrate digestion by inhibitors of digestive enzymes in the gut is seen as a novel approach to diabetes treatment as it provides a way to reduce hyperglycemia (47, 48).

In this study, the α-glycosidase inhibitory activity of the derivatives was determined against the yeast form of this enzyme (Table 1). Enzyme inhibitory results indicated that compounds tested (K_I values = 9.69±1.33 - 111.51±10.66 nM) against α-glycosidase showed better potency than reference acarbose (K_I value = 12600±780 nM. The most active α-glycosidase inhibitors were **2a** and **2d,** with K_I values of 9.69±1.33 and 24.65±5.74 nM. All of the compounds were more potent inhibitors than reference acarbose towards α-amylase. Among them, compound **2a** showed remarkable inhibition with an IC_{50} value of 98.13 nM. Based on the IC_{50} values, α-glycosidase enzyme inhibition studies of the compounds released that 'compounds' IC_{50} values varied in the 8.37-99.35 nM range. Compared to the standard used, the most effective antidiabetic activity and their IC_{50} values were **2a** (8.37 nM), **2d** (27.58 nM), **1d** (46.85 nM), **1c** (57.21 nM) and **2c** (60.48 nM). The results also demonstrated that all these compounds (IC_{50} values = 98.13 – 507.32 nM) showed better inhibitory potency than acarbose (IC_{50} value = 10000 nM) against α-amylase. Therefore, **2a** could be considered both α-glycosidase and α-amylase enzyme inhibitors in this study.

Table 1: α-glycosidase (α-Gly) and α-amylase (α-Amy), acetylcholinesterase (AChE), and butyrylcholinesterase (BChE) enzymes inhibition effects of the compounds.

Compounds	IC_{50} (nM)								K_I (nM)		
	AChE	r^2	BChE	r^2	α-Gly	r^2	α-Amy	r^2	AChE	BChE	α-Gly
1a	41.04	0.9416	234.57	0.9534	61.27	0.9885	395.47	0.9302	51.57±13.85	193.26±14.26	75.42±16.52
1b	71.26	0.9369	129.41	0.9378	99.35	0.9656	507.32	0.9376	88.21±8.32	114.31±8.01	111.51±10.66
1c	93.85	0.9631	105.91	0.9147	57.21	0.9221	283.24	0.9728	78.98±17.46	95.88±8.28	55.31±8.54
1d	53.27	0.9725	213.85	0.988	46.85	0.9485	244.51	0.9057	41.56±6.34	222.04±35.43	51.26±8.75
2a	70.4	0.9621	288.21	0.9233	8.37	0.9324	98.13	0.9629	64.47±9.01	266.74±46.91	9.69±1.33
2c	33.27	0.9354	106.52	0.9764	60.48	0.9054	398.3	0.9714	45.98±10.45	92.18±10.25	62.45±9.83
2d	46.21	0.9606	412.52	0.9361	27.58	0.9344	112.54	0.9248	50.25±7.71	419.46±58.12	24.65±5.74
TAC*	244.94	0.9723	216.40	0.9888	-	-	-	-	201.85±22.54	187.32±34.77	-
ACR**	-	-			22800	0.9505	10000	0.9724	-		12600±780

*Tacrine (TAC) was used as a control for ChEs.
**Acarbose (ACR) was used as a control for α-glycosidase and α-amylase enzymes.

3.3. Basic structure-activity relationships (SARs)

Basic SARs discussion based on compounds' K_I values against AChE and BChE enzymes was given as follows. Initially, when inhibitory activities of thiourea substituted derivatives **1a–d** towards AChE were considered, compounds **1d**, bearing 4,6-dimethylpyrimidin-2-yl were found to be more effective inhibitors than other pyrimidine analogs **1b** and **1c**. Moreover, compound **1d** was also approximately five times more potent inhibitor than reference tacrine. Among pyrimidine derivatives, it could be expressed that substituting the additional methyl groups on the ring led to an increasing AChE inhibitory effect. However, it could be seen from K_I values non-substituted primary 4-sulfamoylphenyl bearing compound **1a** (51.57 nM) has similar inhibitory potency on AChE when compared with **1d** (41.56 nM). These interesting results showed that the replacement of hydrogen atoms on the sulfamoyl group with a bigger size 4,6-dimethylpyrimidin-2-yl moiety did not increase inhibitory potency magnificently, while pyrimidin-2-yl and 4-methylpyrimidin-2-yl bearing compounds decreased inhibitory potency compared to **1a.**

For inhibitory effects of **1a–d** against BChE, the most potent compound was **1c** having 4-methylpyrimidin-2-yl, among others, and it was found two times more potent than tacrine. In contrast to AChE results, compound **1c** having a mono methyl group, increased inhibitory potency compared to non-substituted **1a** and **1d**. Furthermore, compounds **1a–d** showed selective AChE inhibition properties compared to BChE.

When AChE inhibition effects of iminothiazolidinone-sulfonamide derivatives **2a, 2c,** and **2d** were examined, compound **2c** having 4-methylpyrimidin-2-yl was the most effective second compound among

all compounds. Converting the compounds from **1a** to **2a** and from **1d** to **2d** decreased AChE inhibitory effects, except for the **1c**-**2c** compound pair**.** It can be also said that converting flexible thiourea moiety into rigid iminothiazolidinone increased the inhibitory ability of compound **2c**. For the effects on BChE, similar to AChE results, converting the compounds from flexible to rigid structure decreased the BChE inhibitory effects of the compounds, except the **1c**-**2c** compound pair since **1c** and **2c** had very similar Ki values. These discrepancies showed that unique amino acid residues of active sides of both ChEs might lead to different molecular interactions. As a result, converting thiourea into iminothiazolidinone is a preferable modification to obtain more potent ChE inhibitors.

Different chemical structures of the compounds also tested remarkably affected α-glycosidase and α-amylase inhibition properties. So, converting flexible compound **1a,** having 4-sulfamoylphenyl, into rigid compound **2a** led to obtaining an eight times more potent α-glycosidase inhibitor. Similarly, compound **2a** was found to be more potent than its flexible analog **1a** towards α-amylase. It may be said that the non-substituted 4-sulfamoylphenyl group was more favorable than pyrimidine analogs towards α-glycosidase in contrast to ChEs inhibitory results. In addition, iminothiazolidinone derivatives were generally more potent towards α-glycosidase and α-amylase enzymes.

According to all bioassay results, some important outputs may be concluded that compound **2a** could be considered the potential antidiabetic agent since it was a dual inhibitor of enzymes targeting diabetes. Compound **2a** was also a promising inhibitor of AChE at 64.47 nM. Also, compound **2a** may be considered for further pharmacological models to investigate if there is any connection or common point between cholinesterase and diabetes pathways. Among the series, while compound **1d** was five times more selective inhibitor of AChE, compound **2c** was a dual inhibitor of AChE and BChE.

3.4. Molecular docking study

A molecular modeling study was conducted to investigate and evaluate the structural how and why relations of these biological activities of the related compounds because the two compounds with the best activity that were synthesized in this study gave good results against the four enzymes. The following studies have been handled within the scope of this primary purpose. Optimizing the compounds primarily in terms of geometry and energy is essential. Because the three-dimensional orientation or placement of each compound evaluated directly affects its biological activity. Energy minimization aims to find a set of coordinates representing the minimum energy conformation for the given structure. In this context, the optimal 3D poses of the optimized compounds (**1a-1d** and **2a, 2c, 2d**) in the study are represented in Figure 5. Figure 5 gives us information about the distance, angle, or torsional angle of each atom in the compound with the surrounding atoms and briefly in the geometric structure. Detailed information on the optimized compounds was also given in Table S1 in the Supplementary file.

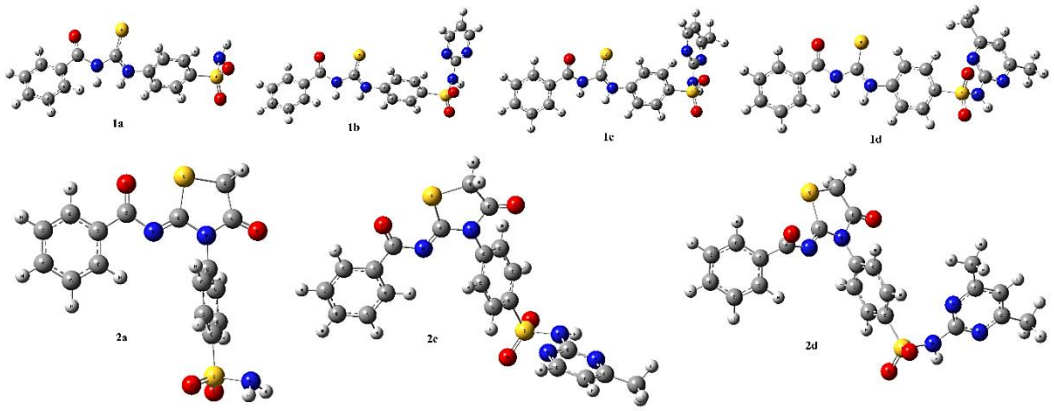

Figure 5: The optimized compounds (**1a-1d** and **2a,2c,2d**) at DFT/B3LYP/6-31G* level using Gaussian09.

In the study, the molecular docking method explains the relationship between the chemical structure of the biological effect of two active compounds showing activity as a result of in vitro analysis for each enzyme.

The two most effective compounds for AChE are compounds **1d** and **2c** (Figure S1). In fact, the binding energy of compound **1d** is -12.43 kcal/mol, while compound **2c** and TAC are -12.32 and -7.37 kcal/mol, respectively. In the meantime, the display of the control compound Tacrine and the orientation in which the two potential compounds interact with the same enzyme is summarized in the overlaid image. The aim is to explain which structural or chemical difference arises from the difference in biological activities of compounds **1c** and **2d** with the target enzyme.

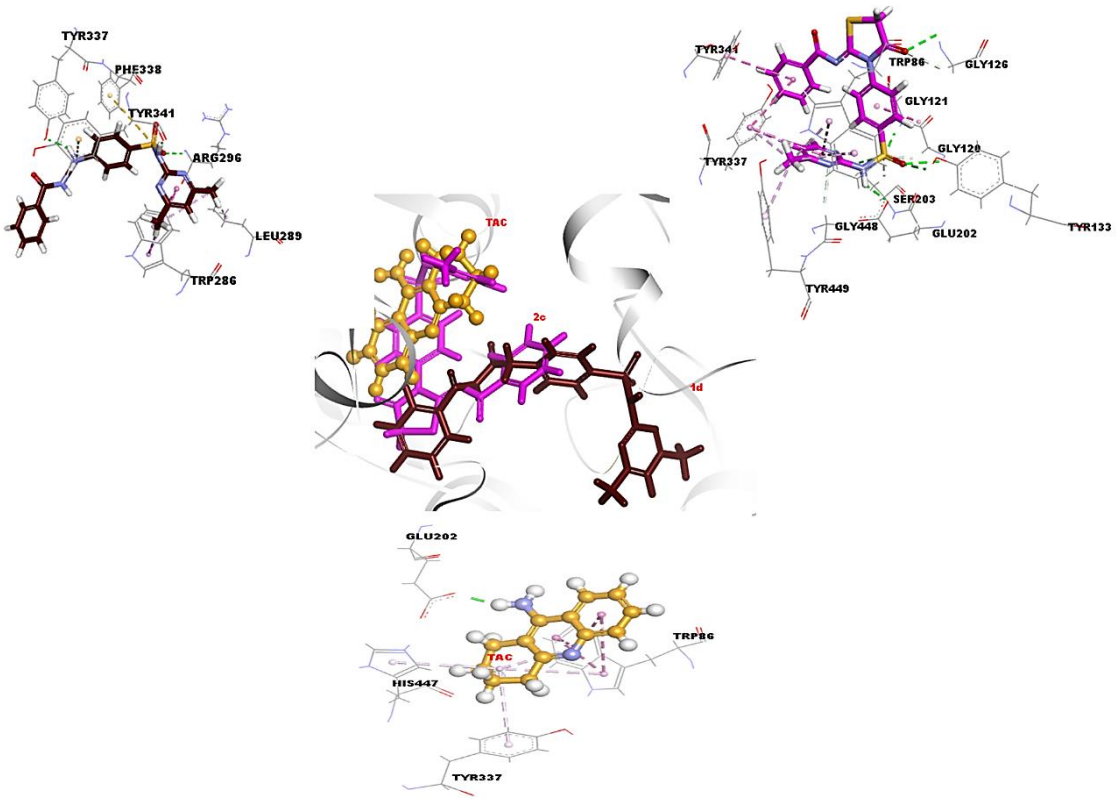

Figure 6: Docking interactions and superimposed form of compound **1d** (brown color, stick form), **2c** (dark pink color, stick form), and TAC (orange, ball, and stick form) with AChE enzyme, respectively.

In this study, the search space of AChE was defined to encompass two distinct binding sites, CAS and PAS. The CAS consisted of amino acids SER203, HIS447, and GLU334, whereas the PAS consisted of amino acids TYR72, ASP74, TYR124, TRP286, and TYR341. Based on Table S2 (Supplementary file), compound **2c** was able to bind to both CAS and PAS simultaneously. The absence of CAS binding was noted in compound **1d**. It exhibited that compound **1d** is bound to TRP286 and TYR341 in the PAS, while compound **2c** is bound to SER203 in the CAS and TYR341 in the PAS.

For BChE, compounds **1c** and **2c** show a more remarkable tendency to bind with the target protein. In particular, compound **2c** has five hydrogen bonds with Gly116, Gly117, Ala199, Ser198, and Ser79 residues in the active site of the related target; two electrostatic interactions with His438 and Asp70; one π-lone pair bond with Trp82, and eight hydrophobic interactions with His438, Trp231, Phe329, Ala328, and Leu286 amino acids. The second-best compound with the target mentioned above model, **1c**, formed eight H-bonds, two electrostatic interactions, and seven hydrophobic interactions. These two compounds interact better than tacrine as a positive compound of BChE. This case is also demonstrated by the binding energy values obtained from the docking calculation (as given in Table 2). As seen in Figure 7, besides the type and number of bonding of the compounds with BChE, the surface areas of the compounds and their volumes in the interaction area have an important place in their effectiveness.

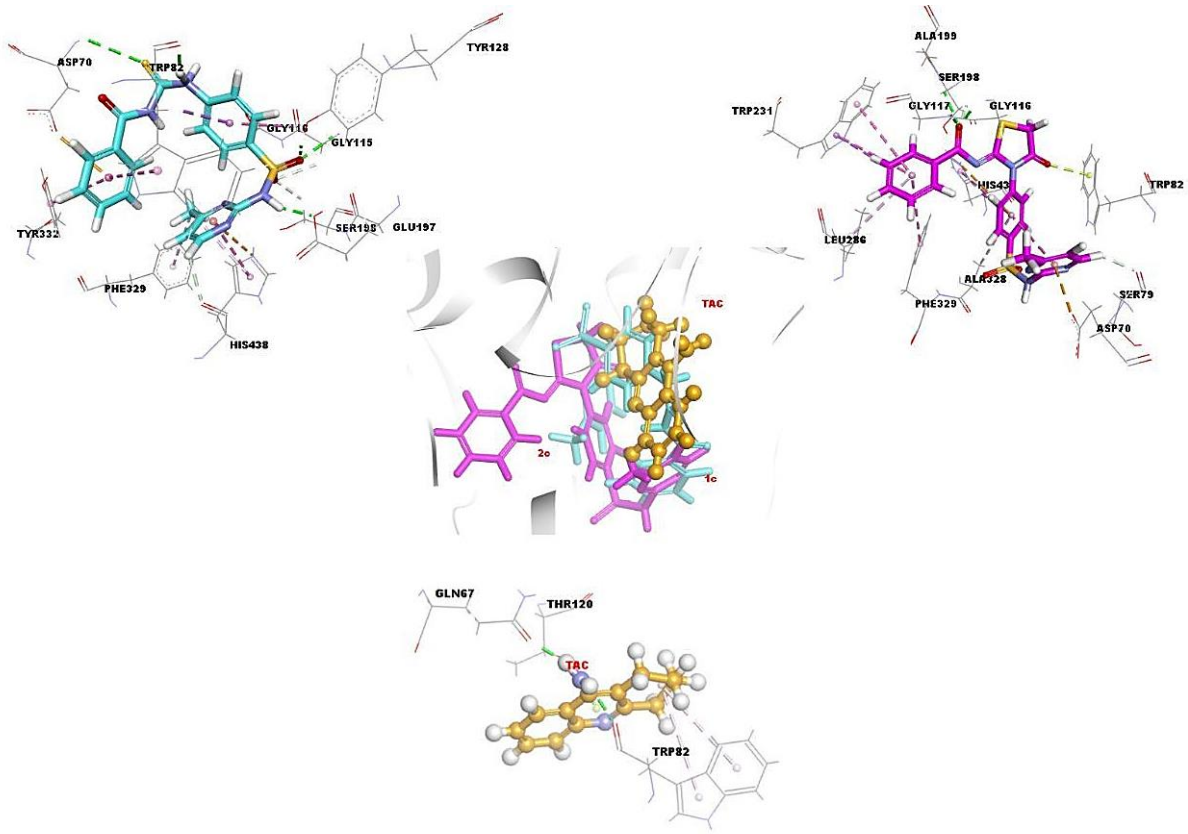

Figure 7: Docking interactions and superimposed form of compound **1c** (turquoise blue color, stick form), **2c** (dark pink color, stick form), and TAC (orange, ball, and stick form) with BChE, respectively.

Table 2: Docking summary of the two potent compounds [**1d** and **1c** for AChE; **1c** and **2c** for BChE; **2a** and **2d** for α-Amy; **2a** and **2d** for α-Gly], TAC and ACR with the target enzymes, respectively.

AChE	**Free Energy of Binding (kcal/mol)**	**RMSD (Å)**
1d	-12.43	0.5946
2c	-12.32	0.8157
TAC	*-7.37*	0.9237
BChE	**Free Energy of Binding (kcal/mol)**	**RMSD (Å)**
1c	-11.02	0.3992
2c	-11.45	1.4512
TAC	*-6.81*	1.5893
α-Amy	**Free Energy of Binding (kcal/mol)**	**RMSD (Å)**
2a	-9.84	0.0923
2d	-8.40	0.4206
ACR	*-5.37*	0.5871
α-Gly	**Free Energy of Binding (kcal/mol)**	**RMSD (Å)**
2a	-11.86	0.1119
2d	-9.57	0.7522
ACR	*-7.53*	1.8320

The acarbose structure, which was chosen as the standard during the molecular docking study, primarily interacted with the model enzyme (Figure S3). Based on the orientation and interactions of the reference compound with the target enzyme, molecular docking studies of two active compounds (**2a** and **2d**) in the in vitro analysis were carried out. The compound **2a** with the Porcine Pancreatic Alpha-Amylase model displayed a binding energy value of -9.84 kcal/mol, and it formed four H-bonds with Arg195, Asp197, Glu233, and His101 residues; three π-sulfur interactions with Trp58, Tyr62, and His299; and three hydrophobic interactions with Trp59, Tyr62, and Trp58. The compound **2d** with α-Amy demonstrated a binding energy value of -8.40 kcal/mol and occurred three H-bonds with His101, His201, and Asp197 amino acids; electrostatic interaction with Asp300; seven hydrophobic interactions with Tyr62, Trp58, His299, Leu162, Ala198, and Ile235 residues (Figure 8). Further, compound **2a** exhibits a better binding affinity than compound **2d** and acarbose (ACR) for α-Amy (BE: -5.37 kcal/mol in Table 2). The findings from the docking are tabulated in detail in Table S2 in the Supplementary file.

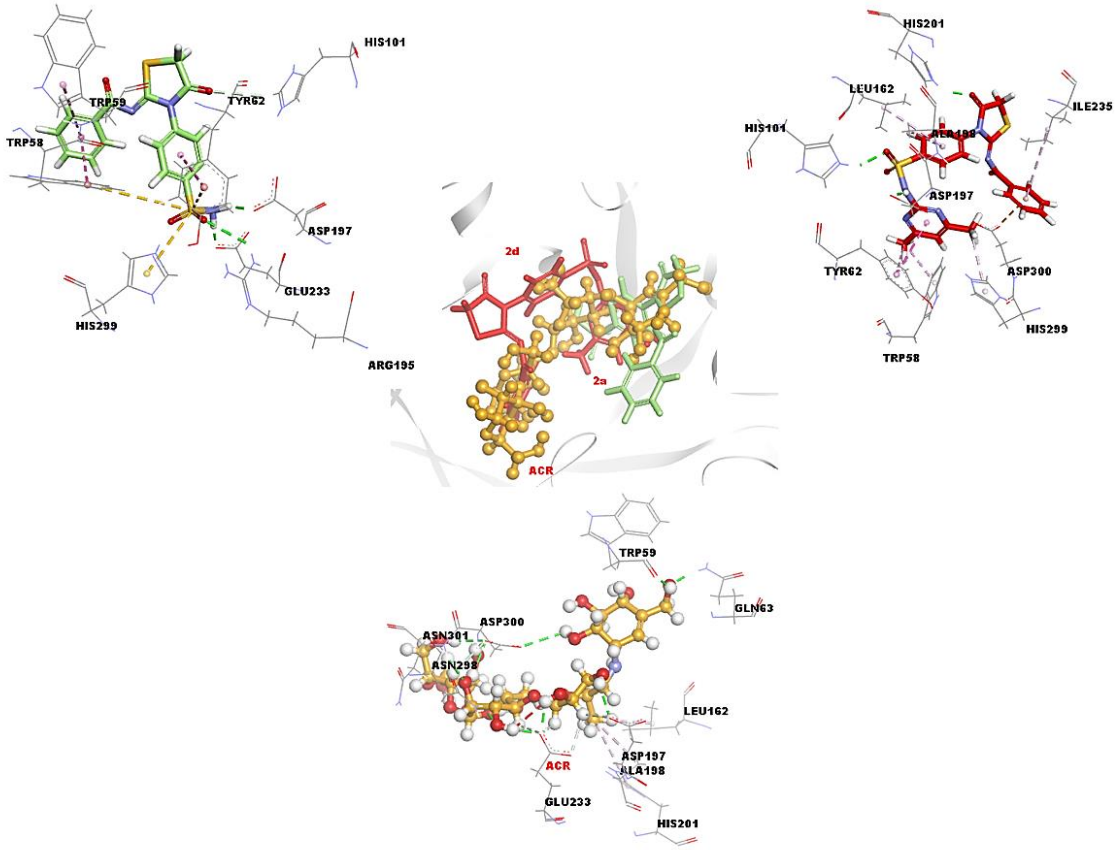

Figure 8: Docking interactions and superimposed form of compound **2a** (light green color, stick form), **2d** (red color, stick form), and ACR (orange, ball, and stick form) with α-Amy, respectively.

Similarly, compounds **2a** and **2d** showing activity for α-Amy also displayed the best activity values with the α-Gly target protein. It was observed that the behaviors of the compounds at α-Gly have a high number of H-bonds and a low number of hydrophobic bonds compared to their behavior in α-Amy, (Figure 9). This is a consequence of the fact that there is more hydrophilic surface than hydrophobic surfaces in the active site of the respective target protein, α-Gly. As a result, the interactions between the compounds mentioned above with α-Gly presented a better binding affinity than their interactions with the α-Amy target, as shown in Table 2.

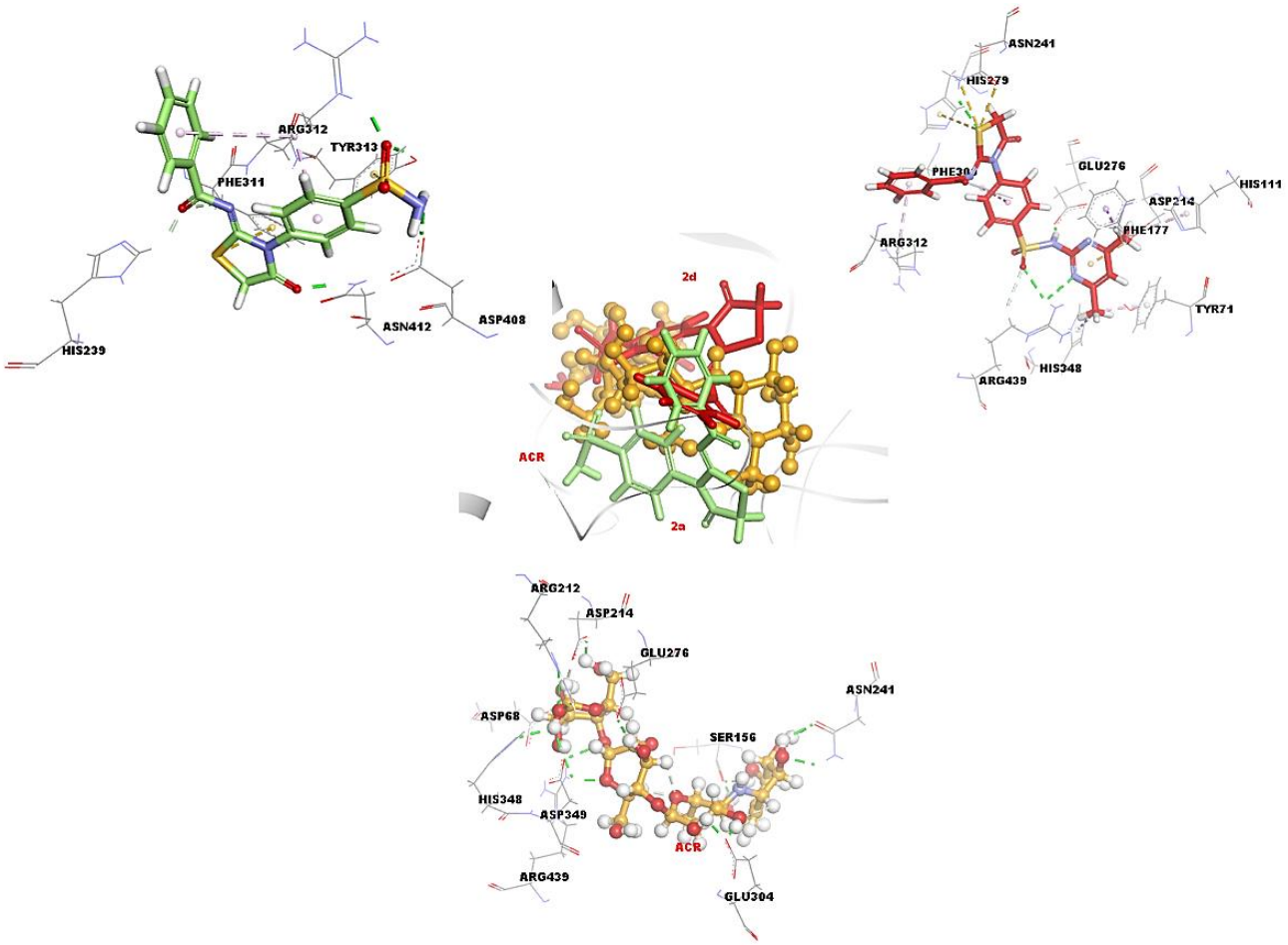

Figure 9: Docking interactions and superimposed form of compound **2a** (light green color, stick form), **2d** (red color, stick form), and **ACR** (orange, ball, and stick form) with α-Gly, respectively.

4. CONCLUSION

In conclusion, thiourea-substituted benzenesulfonamides (**1a–d**) and iminothiazolidinone derivatives (**2a, 2c, 2d**) were evaluated as potent AChE, BChE, α-Gly, and α-Amy inhibitors. Compounds showed inhibitory enzyme effects at the nanomolar level. According to all bioassay results, some important outputs concluded that compound 2a could be considered the potential antidiabetic agent since it was a dual inhibitor of enzymes targeting diabetes. Compound **2a** was also a promising inhibitor of AChE at 64.47 nM. Therefore, compound **2a** may be considered for further pharmacological models. Among the series, while compound **1d** was five times more selective inhibitor of AChE, but compound 2c could be considered a dual inhibitor of AChE and BChE at lower concentrations. The binding energy of the potent compounds was found to be more favorable than references towards all enzymes. Molecular docking studies revealed remarkable interactions between ligands and enzymes. Lead compounds having promising bioactivities could be used to design more potent compounds.

5. CONFLICT OF INTEREST

The authors report no conflict of interest and are responsible for the contents and authoring of the present paper.

6. ACKNOWLEDGMENTS

The authors would like to thank Ataturk University for financial support (Project Number: TAB-8919) and C. Kazaz (Prof. Dr., Ataturk University), B. Anil (Ph.D., Ataturk University), Serkan Levent (M.Sc. Anadolu University) and Mustafa Gul (Prof. Dr. Ataturk University) for their supports.

7. REFERENCES

1. Sadashiva CT, Narendra Sharath Chandra JN, Kavitha CV, Thimmegowda A, Subhash MN, Rangappa KS. Synthesis and pharmacological evaluation of novel N-alkyl/aryl substituted thiazolidinone arecoline analogues as muscarinic receptor 1 agonist in Alzheimer's dementia models. Eur J Med Chem [Internet]. 2009 Dec 1;44(12):4848–54. Available from: <URL>.

2. Genc Bilgicli H, Taslimi P, Akyuz B, Tuzun B, Gulcin İ. Synthesis, characterization, biological evaluation, and molecular docking studies of some piperonyl-

based 4-thiazolidinone derivatives. Arch Pharm (Weinheim) [Internet]. 2020 Jan 28;353(1):1900304. Available from: <URL>.

3. Zhu J, Wang L-N, Cai R, Geng S-Q, Dong Y-F, Liu Y-M. Design, synthesis, evaluation and molecular modeling study of 4-N-phenylaminoquinolines for Alzheimer disease treatment. Bioorg Med Chem Lett [Internet]. 2019 Jun 1;29(11):1325–9. Available from: <URL>.

4. Wilkinson DG, Francis PT, Schwam E, Payne-Parrish J. Cholinesterase Inhibitors Used in the Treatment of Alzheimer's Disease. Drugs Aging [Internet]. 2004 Aug 31;21(7):453–78. Available from: <URL>.

5. Avogaro A, Fadini GP. The Effects of Dipeptidyl Peptidase-4 Inhibition on Microvascular Diabetes Complications. Diabetes Care [Internet]. 2014 Oct 1;37(10):2884–94. Available from: <URL>.

6. Danaei G, Finucane MM, Lu Y, Singh GM, Cowan MJ, Paciorek CJ, et al. National, regional, and global trends in fasting plasma glucose and diabetes prevalence since 1980: systematic analysis of health examination surveys and epidemiological studies with 370 country-years and 2·7 million participants. Lancet [Internet]. 2011 Jul 2;378(9785):31–40. Available from: <URL>.

7. Poovitha S, Parani M. In vitro and in vivo α-amylase and α-glucosidase inhibiting activities of the protein extracts from two varieties of bitter gourd (Momordica charantia L.). BMC Complement Altern Med [Internet]. 2016 Jul 18;16(S1):185. Available from: <URL>.

8. Min SW, Han JS. Polyopes lancifolia Extract, a Potent α-Glucosidase Inhibitor, Alleviates Postprandial Hyperglycemia in Diabetic Mice. Prev Nutr Food Sci [Internet]. 2014 Mar 31;19(1):5–9. Available from: <URL>.

9. Jo S-H, Cho C-Y, Lee J-Y, Ha K-S, Kwon Y-I, Apostolidis E. In vitro and in vivo reduction of post-prandial blood glucose levels by ethyl alcohol and water Zingiber mioga extracts through the inhibition of carbohydrate hydrolyzing enzymes. BMC Complement Altern Med [Internet]. 2016 Dec 31;16(1):111. Available from: <URL>.

10. Zhang B, Xing Y, Wen C, Yu X, Sun W, Xiu Z, et al. Pentacyclic triterpenes as α-glucosidase and α-amylase inhibitors: Structure-activity relationships and the synergism with acarbose. Bioorg Med Chem Lett [Internet]. 2017 Nov 15;27(22):5065–70. Available from: <URL>.

11. Cheng AYY. Oral antihyperglycemic therapy for type 2 diabetes mellitus. Can Med Assoc J [Internet]. 2005 Jan 18;172(2):213–26. Available from: <URL>.

12. Levetan C. Oral antidiabetic agents in type 2 diabetes. Curr Med Res Opin [Internet]. 2007 Apr 1;23(4):945–52. Available from: <URL>.

13. Oz Gul O, Cinkilic N, Gul CB, Cander S, Vatan O, Ersoy C, et al. Comparative genotoxic and cytotoxic effects of the oral antidiabetic drugs sitagliptin, rosiglitazone, and pioglitazone in patients with type-2 diabetes: A cross-sectional, observational pilot study. Mutat Res Toxicol Environ Mutagen [Internet]. 2013 Sep 18;757(1):31–5. Available from: <URL>.

14. Wang S-L, Dong W-B, Dong X-L, Zhu W-M, Wang F-F, Han F, et al. Comparison of twelve single-drug regimens for the treatment of type 2 diabetes mellitus. Oncotarget [Internet]. 2017 Sep 22;8(42):72700–13. Available from: <URL>.

15. Brands AMA, Biessels GJ, de Haan EHF, Kappelle LJ, Kessels RPC. The Effects of Type 1 Diabetes on Cognitive Performance. Diabetes Care [Internet]. 2005 Mar 1;28(3):726–35. Available from: <URL>.

16. Butterfield DA, Di Domenico F, Barone E. Elevated risk of type 2 diabetes for development of Alzheimer disease: A key role for oxidative stress in brain. Biochim Biophys Acta - Mol Basis Dis [Internet]. 2014 Sep;1842(9):1693–706. Available from: <URL>.

17. Zhang J, Chen C, Hua S, Liao H, Wang M, Xiong Y, et al. An updated meta-analysis of cohort studies: Diabetes and risk of Alzheimer's disease. Diabetes Res Clin Pract [Internet]. 2017 Feb 1;124:41–7. Available from: <URL>.

18. Roriz-Filho JS, Sá-Roriz TM, Rosset I, Camozzato AL, Santos AC, Chaves MLF, et al. (Pre)diabetes, brain aging, and cognition. Biochim Biophys Acta - Mol Basis Dis [Internet]. 2009 May 1;1792(5):432–43. Available from: <URL>.

19. Biessels GJ, Staekenborg S, Brunner E, Brayne C, Scheltens P. Risk of dementia in diabetes mellitus: a systematic review. Lancet Neurol [Internet]. 2006 Jan 1;5(1):64–74. Available from: <URL>.

20. Li Z, Zhang W, Sima AAF. Alzheimer-Like Changes in Rat Models of Spontaneous Diabetes. Diabetes [Internet]. 2007 Jul 1;56(7):1817–24. Available from: <URL>.

21. Arab L, Sadeghi R, G. Walker D, Lue L-F, N. Sabbagh M. Consequences of aberrant insulin regulation in the brain: Can treating diabetes be effective for alzheimers disease. Curr Neuropharmacol [Internet]. 2011 Dec 1;9(4):693–705. Available from: <URL>.

22. Maher PA, Schubert DR. Metabolic links between diabetes and Alzheimer's disease. Expert Rev Neurother [Internet]. 2009 May 9;9(5):617–30. Available from: <URL>.

23. Jolivalt CG, Hurford R, Lee CA, Dumaop W, Rockenstein E, Masliah E. Type 1 diabetes exaggerates features of Alzheimer's disease in APP transgenic mice. Exp Neurol [Internet]. 2010 Jun 1;223(2):422–31. Available from: <URL>.

24. Li Y-S, Hu D-K, Zhao D-S, Liu X-Y, Jin H-W, Song G-P, et al. Design, synthesis and biological evaluation

of 2,4-disubstituted oxazole derivatives as potential PDE4 inhibitors. Bioorg Med Chem [Internet]. 2017 Mar 15;25(6):1852–9. Available from: <URL>.

25. Rouf A, Tanyeli C. Bioactive thiazole and benzothiazole derivatives. Eur J Med Chem [Internet]. 2015 Jun 5;97(1):911–27. Available from: <URL>.

26. Jain AK, Vaidya A, Ravichandran V, Kashaw SK, Agrawal RK. Recent developments and biological activities of thiazolidinone derivatives: A review. Bioorg Med Chem [Internet]. 2012 Jun 1;20(11):3378–95. Available from: <URL>.

27. Hemaida AY, Hassan GS, Maarouf AR, Joubert J, El-Emam AA. Synthesis and biological evaluation of thiazole-based derivatives as potential acetylcholinesterase inhibitors. ACS Omega [Internet]. 2021 Jul 27;6(29):19202–11. Available from: <URL>.

28. Markowicz-Piasecka M, Huttunen KM, Sikora J. Metformin and its sulphonamide derivative simultaneously potentiateanti-cholinesterase activity of donepezil and inhibit beta-amyloid aggregation. J Enzyme Inhib Med Chem [Internet]. 2018 Jan 1;33(1):1309–22. Available from: <URL>.

29. Yamali C, Gul HI, Kazaz C, Levent S, Gulcin I. Synthesis, structure elucidation, and in vitro pharmacological evaluation of novel polyfluoro substituted pyrazoline type sulfonamides as multi-target agents for inhibition of acetylcholinesterase and carbonic anhydrase I and II enzymes. Bioorg Chem [Internet]. 2020 Mar 1;96:103627. Available from: <URL>.

30. Yamali C, Gul HI, Ece A, Taslimi P, Gulcin I. Synthesis, molecular modeling, and biological evaluation of 4-[5-aryl-3-(thiophen-2-yl)-4,5-dihydro-1 *H* -pyrazol-1-yl] benzenesulfonamides toward acetylcholinesterase, carbonic anhydrase I and II enzymes. Chem Biol Drug Des [Internet]. 2018 Apr 1;91(4):854–66. Available from: <URL>.

31. Tugrak M, Gul HI, Demir Y, Gulcin I. Synthesis of benzamide derivatives with thiourea-substituted benzenesulfonamides as carbonic anhydrase inhibitors. Arch Pharm (Weinheim) [Internet]. 2021 Feb 12;354(2):e2000230. Available from: <URL>.

32. Ellman GL, Courtney KD, Andres V, Featherstone RM. A new and rapid colorimetric determination of acetylcholinesterase activity. Biochem Pharmacol [Internet]. 1961 Jul 1;7(2):88–95. Available from: <URL>.

33. Cetin Cakmak K, Gülçin İ. Anticholinergic and antioxidant activities of usnic acid-an activity-structure insight. Toxicol Reports [Internet]. 2019 Jan 1;6:1273–80. Available from: <URL>.

34. Buldurun K, Turan N, Bursal E, Aras A, Mantarcı A, Çolak N, et al. Synthesis, characterization, powder X-ray diffraction analysis, thermal stability, antioxidant properties and enzyme inhibitions of M(II)-Schiff base ligand complexes. J Biomol Struct Dyn [Internet]. 2021 Nov 22;39(17):6480–7. Available from: <URL>.

35. Behçet A, Çağlılar T, Barut Celepci D, Aktaş A, Taslimi P, Gök Y, et al. Synthesis, characterization and crystal structure of 2-(4-hydroxyphenyl)ethyl and 2-(4-nitrophenyl)ethyl Substituted Benzimidazole Bromide Salts: Their inhibitory properties against carbonic anhydrase and acetylcholinesterase. J Mol Struct [Internet]. 2018 Oct 15;1170:160–9. Available from: <URL>.

36. Tao Y, Zhang Y, Cheng Y, Wang Y. Rapid screening and identification of *α* -glucosidase inhibitors from mulberry leaves using enzyme-immobilized magnetic beads coupled with HPLC/MS and NMR. Biomed Chromatogr [Internet]. 2013 Feb;27(2):148–55. Available from: <URL>.

37. Bal S, Demirci Ö, Şen B, Taşkın Tok T, Taslimi P, Aktaş A, et al. Silver *N* -heterocyclic carbene complexes bearing fluorinated benzyl group: Synthesis, characterization, crystal structure, computational studies, and inhibitory properties against some metabolic enzymes. Appl Organomet Chem [Internet]. 2021 Sep 20;35(9):e6312. Available from: <URL>.

38. Xiao Z, Storms R, Tsang A. A quantitative starch–iodine method for measuring alpha-amylase and glucoamylase activities. Anal Biochem [Internet]. 2006 Apr 1;351(1):146–8. Available from: <URL>.

39. Gaussian 09, revision E.01, MJ Frisch, WW Trucks, HB Schlegel, GE Scuseria, MA Robb, JR Cheeseman, G Scalmani, V. Barone, B. Mennucci, G.A.e.a. Petersson, Gaussian, Inc,. Wallingford CT; 2009. p. S162-173.

40. Bank RPD RCSB PDB:Homepage. BRRP [Internet]. 2021 [cited 2021 May 24]. Available from: <URL>.

41. Accelrys Software Inc. Discovery studio modeling environment, Release 3.5 Accelrys Software Inc. San Diego; 2013.

42. Mugaranja KP, Kulal A. Alpha glucosidase inhibition activity of phenolic fraction from Simarouba glauca: An in-vitro, in-silico and kinetic study. Heliyon [Internet]. 2020 Jul 1;6(7):e04392. Available from: <URL>.

43. Brooks BR, Bruccoleri RE, Olafson BD, States DJ, Swaminathan S, Karplus M. CHARMM: A program for macromolecular energy, minimization, and dynamics calculations. J Comput Chem [Internet]. 1983 Jun 1;4(2):187–217. Available from: <URL>.

44. Trott O, Olson AJ. AutoDock Vina: Improving the speed and accuracy of docking with a new scoring function, efficient optimization, and multithreading. J Comput Chem [Internet]. 2009 Jan 1;31(2):455–61. Available from: <URL>.

45. Huseynova M, Medjidov A, Taslimi P, Aliyeva M. Synthesis, characterization, crystal structure of the coordination polymer Zn(II) with thiosemicarbazone

of glyoxalic acid and their inhibitory properties against some metabolic enzymes. Bioorg Chem [Internet]. 2019 Mar 1;83:55–62. Available from: <URL>.

46. Biçer A, Taslimi P, Yakalı G, Gülçin I, Serdar Gültekin M, Turgut Cin G. Synthesis, characterization, crystal structure of novel bis-thiomethylcyclohexanone derivatives and their inhibitory properties against some metabolic enzymes. Bioorg Chem [Internet]. 2019 Feb 1;82:393–404. Available from: <URL>.

47. Demir Y, Taslimi P, Ozaslan MS, Oztaskin N, Çetinkaya Y, Gulçin İ, et al. Antidiabetic potential: In vitro inhibition effects of bromophenol and diarylmethanones derivatives on metabolic enzymes. Arch Pharm (Weinheim) [Internet]. 2018 Dec 1;351(12):e1800263. Available from: <URL>.

48. Gulçin İ, Taslimi P, Aygün A, Sadeghian N, Bastem E, Kufrevioglu OI, et al. Antidiabetic and antiparasitic potentials: Inhibition effects of some natural antioxidant compounds on α-glycosidase, α-amylase and human glutathione S-transferase enzymes. Int J Biol Macromol [Internet]. 2018 Nov 1;119:741–6. Available from: <URL>.

SUPPLEMENTARY MATERIAL

Molecular docking studies and biological activities of benzenesulfonamide-based thiourea and thiazolidinone derivatives targeting cholinesterases, α-glucosidase, and α-amylase enzymes

Mehtap Tugrak Sakarya[1*], Halise Inci Gul[2], Cem Yamali[3], Parham Taslimi[4], Tugba Taskin Tok[5,6]

[1]Gaziosmanpasa University, Department of Pharmaceutical Chemistry, Tokat, Turkey.
[2]Ataturk University, Department of Pharmaceutical Chemistry, Erzurum, Turkey.
[3]Cukurova University, Department of Basic Pharmaceutical Sciences, Adana, Turkey.
[4]Bartin University, Department of Biotechnology, Faculty of Science, Bartin, Turkey.
[5]Gaziantep University, Department of Chemistry, Gaziantep, Turkey.
[6]Gaziantep University, Department of Bioinformatics and Computational Biology, Gaziantep, Turkey.

Table S1. Data of the optimized structures (**1a-1d** and **2a,2c,2d**) at DFT/B3LYP/6-31G* basis set using Gaussian 09.

Compound 1a					
			Coordinates (Angstroms)		
Center Number	Atomic Number	Atomic Type	X	Y	Z
1	6	0	-4.905464	-0.088218	-0.089881
2	6	0	-3.702342	0.758615	-0.385636
3	7	0	-2.479523	0.16078	-0.025686
4	6	0	-1.211958	0.760437	0.04181
5	7	0	-0.250668	-0.182371	-0.266702
6	6	0	1.153215	-0.157642	-0.150076
7	8	0	-3.77946	1.840293	-0.929724
8	16	0	-0.956246	2.336451	0.460856
9	6	0	1.866096	-1.051244	-0.969633
10	6	0	3.248831	-1.140544	-0.888835
11	6	0	3.931358	-0.327789	0.017979
12	6	0	3.23618	0.550127	0.849285
13	6	0	1.849034	0.640644	0.769803
14	6	0	-4.939998	-1.055699	0.925382
15	6	0	-6.102387	-1.791948	1.154985
16	6	0	-7.235983	-1.570365	0.371208
17	6	0	-7.211224	-0.599039	-0.633518
18	6	0	-6.055372	0.143629	-0.857913
19	16	0	5.713324	-0.430611	0.124339
20	8	0	6.116765	-1.779315	-0.285737
21	8	0	6.110139	0.146808	1.412768
22	7	0	6.241612	0.602087	-1.117964
23	1	0	-2.51952	-0.82907	0.183877
24	1	0	-0.592581	-0.962989	-0.815748
25	1	0	1.329345	-1.679957	-1.676888

26	1	0	3.79422	-1.839326	-1.513738
27	1	0	3.778237	1.149701	1.572565
28	1	0	1.312277	1.323248	1.412497
29	1	0	-4.079969	-1.209125	1.572523
30	1	0	-6.125117	-2.529618	1.952138
31	1	0	-8.139804	-2.146639	0.548973
32	1	0	-8.095221	-0.419318	-1.238834
33	1	0	-6.019936	0.911845	-1.623379
34	1	0	6.961759	0.119303	-1.652495
35	1	0	6.603674	1.466978	-0.720354

Compound 1b					
			Coordinates (Angstroms)		
Center Number	Atomic Number	Atomic Type	X	Y	Z
1	6	0	6.161601	0.285754	0.16655
2	6	0	4.82776	0.963087	0.285433
3	7	0	3.733811	0.127119	-0.008313
4	6	0	2.393582	0.497718	-0.205923
5	7	0	1.574433	-0.522426	0.235837
6	6	0	0.191443	-0.747221	0.089498
7	8	0	4.706909	2.11419	0.649483
8	16	0	1.924203	1.924142	-0.891645
9	6	0	-0.398044	-1.628333	1.014171
10	6	0	-1.743984	-1.955312	0.924044
11	6	0	-2.511326	-1.394103	-0.098543
12	6	0	-1.938773	-0.530227	-1.032436
13	6	0	-0.588864	-0.203832	-0.942631
14	6	0	6.401232	-0.806735	-0.680106
15	6	0	7.67377	-1.373637	-0.752285
16	6	0	8.713812	-0.856809	0.022097
17	6	0	8.483794	0.239522	0.857969
18	6	0	7.217069	0.813102	0.924013
19	8	0	-4.235465	-1.836872	-0.228527
20	8	0	-4.447338	-3.097488	0.487648
21	7	0	-4.656194	-1.660968	-1.614556
22	1	0	-5.042411	-0.719283	0.783879
23	1	0	3.937999	-0.863642	-0.053603
24	1	0	2.009695	-1.142937	0.909047
25	1	0	0.205465	-2.059631	1.809991
26	1	0	-2.195122	-2.645088	1.628712
27	1	0	-2.55097	-0.115234	-1.823567
28	1	0	-0.145748	0.469826	-1.661348
29	1	0	5.61264	-1.192549	-1.321416
30	1	0	7.854291	-2.210892	-1.420521
31	1	0	9.703789	-1.301275	-0.032558
32	1	0	9.294127	0.648424	1.454905

33	1	0	7.021085	1.673249	1.555762
34	1	0	-5.660158	-1.181466	1.444181
35	6	0	-5.378573	0.592046	0.467583
36	6	0	-6.696922	2.374223	0.926651
37	6	0	-4.994631	2.484067	-0.710251
38	6	0	-6.025279	3.131248	-0.032617
39	1	0	-7.514221	2.796903	1.508612
40	1	0	-4.4122	2.996873	-1.473577
41	1	0	-6.288254	4.16252	-0.237919
42	7	0	-6.391347	1.100948	1.18644
43	7	0	-4.652378	1.215842	-0.466965

Compound 1c					
			Coordinates (Angstroms)		
Center Number	Atomic Number	Atomic Type	X	Y	Z
1	6	0	-6.181604	0.106647	-0.57759
2	6	0	-4.733041	-0.182091	-0.353459
3	7	0	-4.099737	0.603553	0.593471
4	6	0	-2.752579	0.620885	1.011199
5	7	0	-1.980576	-0.29093	0.37879
6	6	0	-0.611572	-0.604912	0.467623
7	8	0	-4.150098	-1.078898	-0.968724
8	16	0	-2.345371	1.739895	2.186499
9	6	0	-0.171694	-1.607126	-0.42018
10	6	0	1.154024	-2.01285	-0.429584
11	6	0	2.054929	-1.411375	0.453278
12	6	0	1.634558	-0.425545	1.344277
13	6	0	0.302457	-0.017116	1.355619
14	6	0	-6.786529	1.332201	-0.258509
15	6	0	-8.144299	1.527975	-0.505203
16	6	0	-8.90836	0.504306	-1.068883
17	6	0	-8.30892	-0.713716	-1.399304
18	6	0	-6.951474	-0.909953	-1.162072
19	16	0	3.752844	-1.962526	0.461465
20	8	0	3.81183	-3.294528	-0.146811
21	8	0	4.323484	-1.694288	1.777534
22	7	0	4.521858	-1.000153	-0.726784
23	1	0	-4.658999	1.259691	1.122358
24	1	0	-2.508464	-0.859002	-0.293889
25	1	0	-0.880841	-2.070706	-1.101391
26	1	0	1.489022	-2.796386	-1.100152
27	1	0	2.349273	0.023292	2.023134
28	1	0	-0.026801	0.744626	2.046993
29	1	0	-6.204417	2.156086	0.145938
30	1	0	-8.602479	2.482597	-0.263862
31	1	0	-9.967305	0.658356	-1.256604

32	1	0	-8.899935	-1.509627	-1.843166
33	1	0	-6.467104	-1.845625	-1.419789
34	1	0	5.043243	-1.56839	-1.387676
35	6	0	5.003262	0.294146	-0.5519
36	6	0	6.45606	1.894156	-1.276755
37	6	0	4.901187	2.296578	0.478808
38	6	0	5.928007	2.777455	-0.328216
39	1	0	4.440469	2.929515	1.235427
40	1	0	6.300028	3.790802	-0.22624
41	7	0	5.993597	0.639711	-1.383988
42	7	0	4.414907	1.056949	0.377108
43	6	0	7.564676	2.285517	-2.216388
44	1	0	8.431915	1.632361	-2.068687
45	1	0	7.241264	2.157927	-3.255385
46	1	0	7.874962	3.323283	-2.067163

Compound 1d					
			Coordinates (Angstroms)		
Center Number	Atomic Number	Atomic Type	X	Y	Z
1	6	0	-6.357565	0.010588	0.529953
2	6	0	-4.888583	0.228924	0.369352
3	7	0	-4.207512	-0.74386	-0.341585
4	6	0	-2.848323	-0.820025	-0.709762
5	7	0	-2.117901	0.240771	-0.299609
6	6	0	-0.761257	0.579743	-0.461191
7	8	0	-4.323669	1.211386	0.857298
8	16	0	-2.377051	-2.178911	-1.565389
9	6	0	-0.345771	1.7305	0.237665
10	6	0	0.964046	2.177445	0.150471
11	6	0	1.87271	1.468972	-0.639998
12	6	0	1.474753	0.336046	-1.34719
13	6	0	0.159076	-0.114391	-1.261436
14	6	0	-6.991884	0.687063	1.582443
15	6	0	-8.359113	0.532605	1.792662
16	6	0	-9.109288	-0.287034	0.945555
17	6	0	-8.488452	-0.948017	-0.116076
18	6	0	-7.117956	-0.802575	-0.324595
19	16	0	3.550965	2.064167	-0.774658
20	8	0	3.568889	3.486262	-0.420301
21	8	0	4.113747	1.581577	-2.032098
22	7	0	4.36126	1.360022	0.554312
23	1	0	-4.71424	-1.572202	-0.624918
24	1	0	-2.666145	0.91031	0.252551
25	1	0	-1.061145	2.276263	0.847751
26	1	0	1.279985	3.072342	0.675074
27	1	0	2.195161	-0.192265	-1.959255

28	1	0	-0.152653	-0.991508	-1.809359
29	1	0	-6.394959	1.326426	2.223864
30	1	0	-8.841031	1.052589	2.615563
31	1	0	-10.177071	-0.404943	1.10769
32	1	0	-9.071456	-1.571159	-0.787851
33	1	0	-6.663253	-1.296256	-1.179466
34	1	0	4.872001	2.053595	1.092336
35	6	0	4.875483	0.065982	0.617842
36	6	0	6.363866	-1.334012	1.610858
37	6	0	4.806707	-2.105917	-0.036762
38	6	0	5.851296	-2.387073	0.847157
39	1	0	6.251732	-3.390941	0.938344
40	7	0	5.877008	-0.090102	1.492763
41	7	0	4.304291	-0.86648	-0.147004
42	7	0	7.484307	-1.526976	2.597306
43	1	0	8.326038	-0.872925	2.344412
44	1	0	7.153132	-1.247187	3.603746
45	1	0	7.83407	-2.562791	2.616199
46	6	0	4.183898	-3.162405	-0.9086
47	1	0	4.607382	-4.151468	-0.71378
48	1	0	3.101794	-3.199295	-0.742117
49	1	0	4.338575	-2.915591	-1.965297

Compound 2a					
			Coordinates (Angstroms)		
Center Number	Atomic Number	Atomic Type	X	Y	Z
1	6	0	-4.708362	-3.637217	-0.078839
2	6	0	-3.577958	-4.454976	-0.176521
3	6	0	-2.302429	-3.886608	-0.20632
4	6	0	-2.152375	-2.502493	-0.13803
5	6	0	-3.283533	-1.678219	-0.039722
6	6	0	-4.56291	-2.25514	-0.011293
7	6	0	-3.171144	-0.196563	0.032779
8	8	0	-4.162494	0.531	0.104144
9	7	0	-1.860159	0.296745	0.014567
10	6	0	-1.68777	1.571186	0.040113
11	7	0	-0.400644	2.110934	0.01772
12	6	0	-0.292924	3.51179	0.006078
13	6	0	-1.664293	4.15729	0.059647
14	16	0	-2.937844	2.836123	0.093961
15	8	0	0.756835	4.112669	-0.039865
16	6	0	0.775489	1.285172	-0.001773
17	6	0	0.995272	0.36193	1.025005
18	6	0	2.142418	-0.424613	1.009175
19	6	0	3.063948	-0.265743	-0.027828
20	6	0	2.850886	0.65271	-1.053827

21	6	0	1.696165	1.433454	-1.039656
22	16	0	4.541581	-1.283722	-0.052434
23	8	0	4.216618	-2.566445	0.577264
24	8	0	5.111916	-1.193445	-1.399975
25	7	0	5.577909	-0.484209	1.028314
26	1	0	-5.700367	-4.079934	-0.056078
27	1	0	-3.692311	-5.534548	-0.229912
28	1	0	-1.424379	-4.521858	-0.283611
29	1	0	-1.167766	-2.049636	-0.162311
30	1	0	-5.425785	-1.601561	0.063893
31	1	0	-1.792832	4.800952	-0.815301
32	1	0	-1.728031	4.783986	0.953897
33	1	0	0.265697	0.251774	1.818581
34	1	0	2.318328	-1.159886	1.786748
35	1	0	3.569987	0.739744	-1.860642
36	1	0	1.512851	2.151822	-1.830113
37	1	0	5.954362	-1.166824	1.683641
38	1	0	6.32483	-0.018748	0.516086

Compound 2c					
			Coordinates (Angstroms)		
Center Number	Atomic Number	Atomic Type	X	Y	Z
1	6	0	-6.0069	-3.639133	0.739185
2	6	0	-4.93079	-4.450642	0.365706
3	6	0	-3.704086	-3.875452	0.026318
4	6	0	-3.548636	-2.490588	0.059555
5	6	0	-4.625253	-1.672663	0.434274
6	6	0	-5.855972	-2.256403	0.773299
7	6	0	-4.505006	-0.190689	0.483508
8	8	0	-5.450216	0.53082	0.805219
9	7	0	-3.242829	0.309647	0.139684
10	6	0	-3.073026	1.58467	0.133062
11	7	0	-1.834984	2.131656	-0.207816
12	6	0	-1.737521	3.532963	-0.229973
13	6	0	-3.053023	4.170722	0.174138
14	16	0	-4.273271	2.842291	0.513136
15	8	0	-0.734797	4.140488	-0.531165
16	6	0	-0.700038	1.312384	-0.536171
17	6	0	-0.221671	0.382236	0.39031
18	6	0	0.884136	-0.40167	0.073515
19	6	0	1.50314	-0.228365	-1.165181
20	6	0	1.033672	0.699779	-2.094592
21	6	0	-0.077809	1.475982	-1.775293
22	16	0	2.904142	-1.255383	-1.605538
23	8	0	2.812075	-2.502263	-0.85348
24	8	0	3.047034	-1.241601	-3.063038

25	7	0	4.263599	-0.352487	-1.103514
26	1	0	-6.961093	-4.087287	1.002478
27	1	0	-5.049606	-5.530729	0.338854
28	1	0	-2.868528	-4.505812	-0.265148
29	1	0	-2.602045	-2.032211	-0.203214
30	1	0	-6.677236	-1.607566	1.059505
31	1	0	-3.39936	4.822068	-0.6334
32	1	0	-2.891346	4.788361	1.062329
33	1	0	-0.720789	0.264469	1.344912
34	1	0	1.275185	-1.128396	0.774465
35	1	0	1.51995	0.797346	-3.058721
36	1	0	-0.4598	2.201654	-2.483718
37	1	0	4.938691	-0.242186	-1.854367
38	6	0	4.796881	-0.307625	0.182949
39	6	0	6.643478	0.092662	1.457593
40	6	0	4.533513	-0.445228	2.417187
41	6	0	5.876405	-0.134571	2.60625
42	1	0	3.877069	-0.630456	3.265748
43	1	0	6.307488	-0.070388	3.59905
44	7	0	3.967546	-0.526869	1.209727
45	7	0	6.098851	-0.002969	0.235556
46	6	0	8.104877	0.44578	1.517963
47	1	0	8.470579	0.483032	2.547639
48	1	0	8.693583	-0.289411	0.958495
49	1	0	8.277049	1.419693	1.046172

Compound 2d					
			Coordinates (Angstroms)		
Center Number	Atomic Number	Atomic Type	X	Y	Z
1	6	0	-7.650499	-1.459049	0.203127
2	6	0	-7.227246	-2.554035	-0.543555
3	6	0	-5.868857	-2.821916	-0.678319
4	6	0	-4.928928	-1.993855	-0.074187
5	6	0	-5.35466	-0.893535	0.671338
6	6	0	-6.718121	-0.629786	0.816125
7	6	0	-4.36931	-0.005798	1.343548
8	8	0	-4.417112	0.359707	2.499719
9	7	0	-3.213692	0.375696	0.573152
10	6	0	-2.955162	1.493852	-0.008666
11	7	0	-1.703108	1.591923	-0.731365
12	6	0	-1.446272	2.896424	-1.283601
13	6	0	-2.623897	3.839135	-1.139993
14	16	0	-3.91549	3.001471	-0.167521
15	8	0	-0.392534	3.155496	-1.827218
16	6	0	-0.634532	0.617918	-0.551924

17	6	0	0.066457	0.534811	0.652835
18	6	0	1.081885	-0.405541	0.788895
19	6	0	1.410848	-1.265906	-0.261501
20	6	0	0.698726	-1.1662	-1.460495
21	6	0	-0.320213	-0.234779	-1.613899
22	16	0	2.686453	-2.485018	-0.074681
23	8	0	2.930428	-2.796178	1.315886
24	8	0	2.476886	-3.585799	-1.00786
25	7	0	4.09796	-1.661489	-0.761111
26	1	0	-8.720021	-1.250984	0.313394
27	1	0	-7.964081	-3.207427	-1.02272
28	1	0	-5.536373	-3.688263	-1.260053
29	1	0	-3.859805	-2.212349	-0.17968
30	1	0	-7.05175	0.224503	1.416719
31	1	0	-3.01177	0.224503	1.416719
32	1	0	-2.315625	4.778854	-0.644403
33	1	0	-0.173829	1.193221	1.496215
34	1	0	1.637743	-0.464353	1.736835
35	1	0	0.937906	-1.840932	-2.294602
36	1	0	-0.862503	-0.175219	-2.565066
37	1	0	4.575184	-2.133797	-1.508776
38	6	0	4.872838	-0.62414	-0.193703
39	6	0	6.858397	0.611975	-0.203009
40	6	0	5.07134	1.141918	1.325649
41	6	0	6.351938	1.410254	0.83022
42	1	0	6.94683	2.231517	1.243435
43	7	0	4.326684	0.126545	0.810707
44	7	0	6.120052	-0.407366	-0.716912
45	6	0	8.21879	0.842032	-0.760956
46	1	0	8.482405	1.907828	-0.730846
47	1	0	8.966992	0.298502	-0.166581
48	1	0	8.314225	0.501631	-1.800858
49	6	0	4.484071	1.949191	2.429271
50	1	0	4.617828	3.022586	2.238608
51	1	0	3.410487	1.763763	2.57146
52	1	0	4.988567	1.715155	3.377273

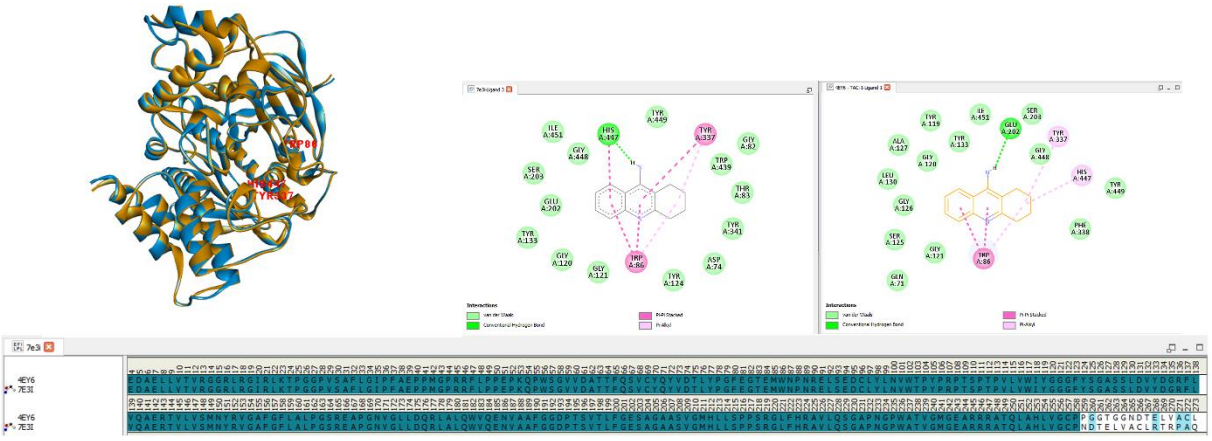

Figure S1. Superimposed structures, sequences of the two Human Acetylcholinesterase models, 7E3I (orange color) and 4EY6 (blue color). 2D docking poses and interactions of Tacrine in the two PDB models.

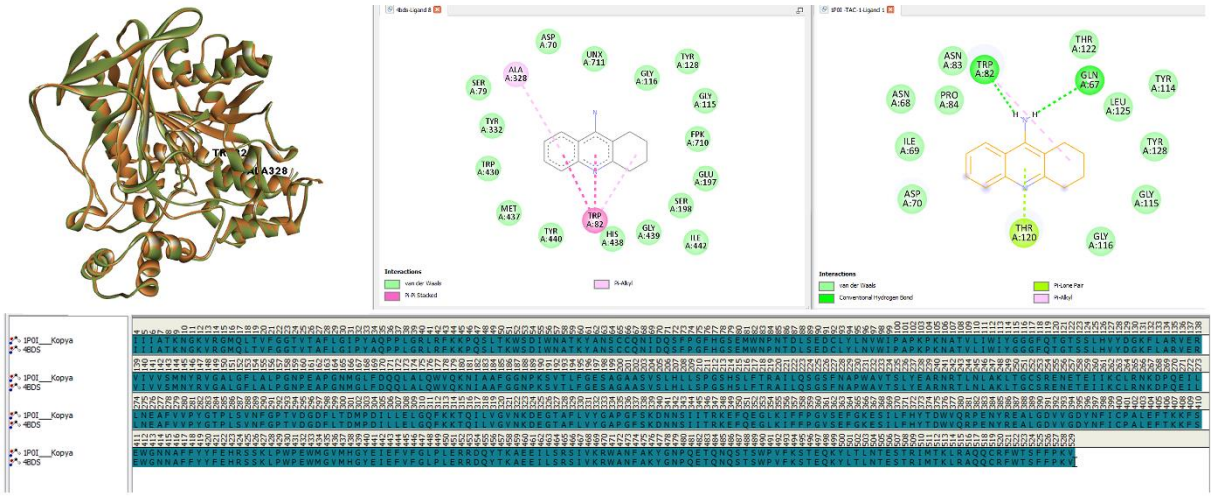

Figure S2. Superimposed structures, sequences of the two Human butyrylcholinesterase models, 4BDS (green color) and 1P0I (orange color). 2D docking poses and interactions of Tacrine in the two PDB models.

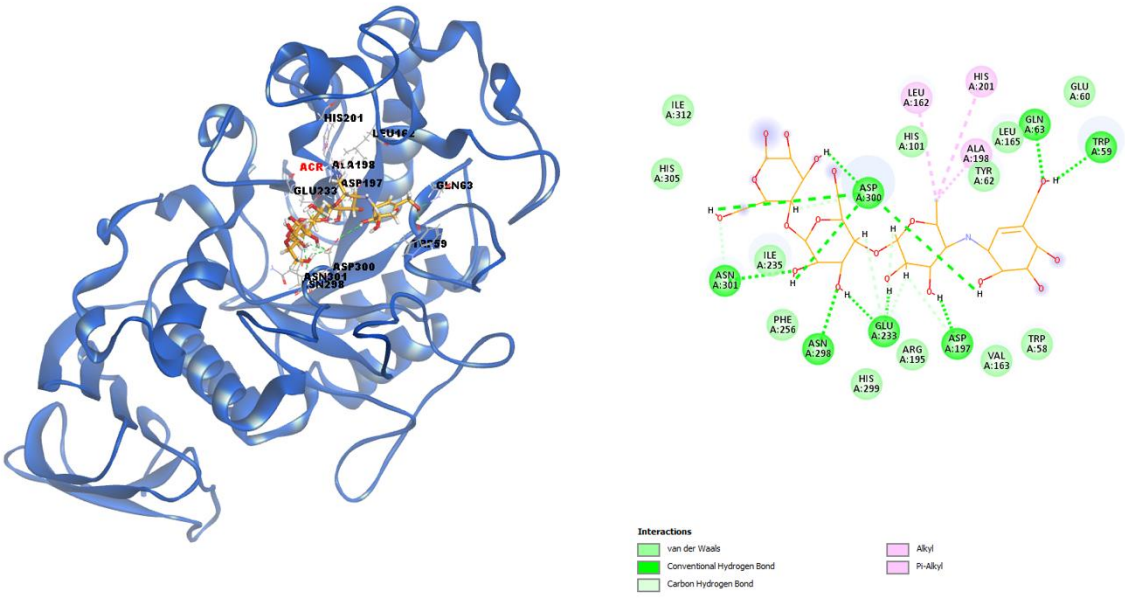

Figure S3. 3D and 2D docking poses and interactions of acarbose in the **Porcine Pancreatic Alpha-Amylase** model (1DHK, blue color).

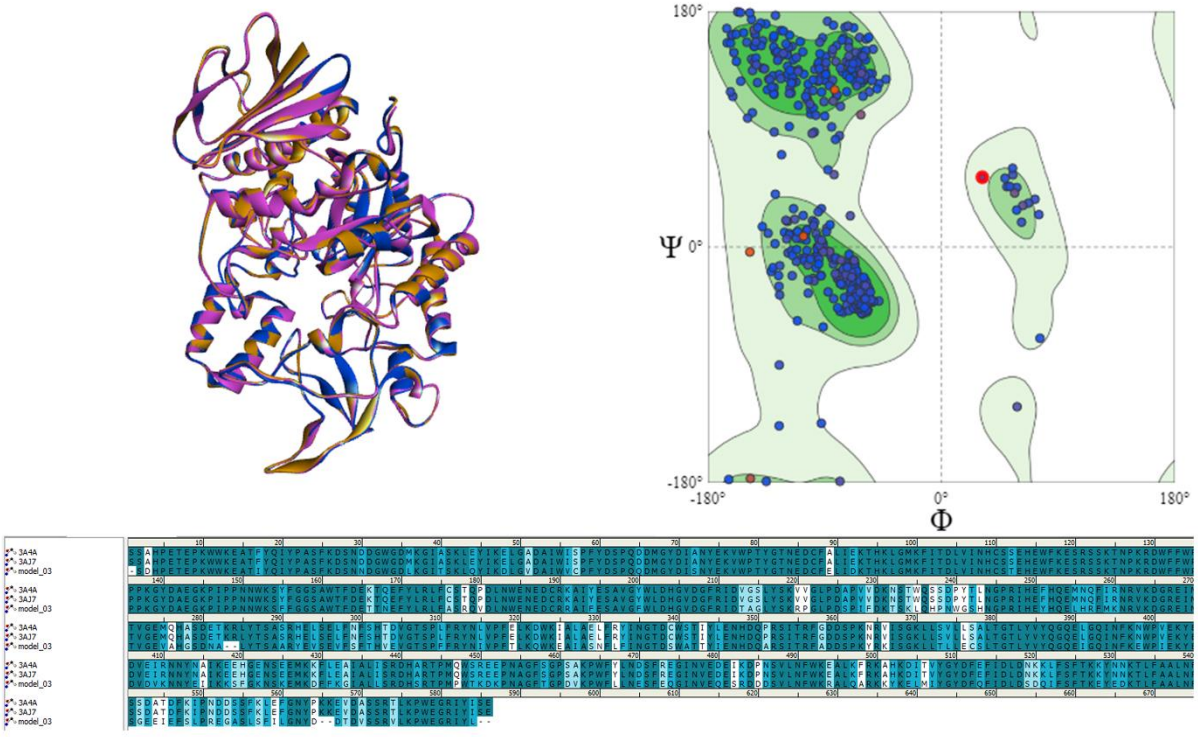

Figure S4. Superimposed structures, sequences of the two isomaltase /α-methylglucosidase from S. cerevisiae models, 3AJ7 (blue color) and 3A4A (orange color) and model3 (pink color). Ramachandran plot for homology model of yeast alpha glucosidase (model 3). The homology model was built and The model was validated and authenticated by Ramachandran plot using DS 3.5 software.

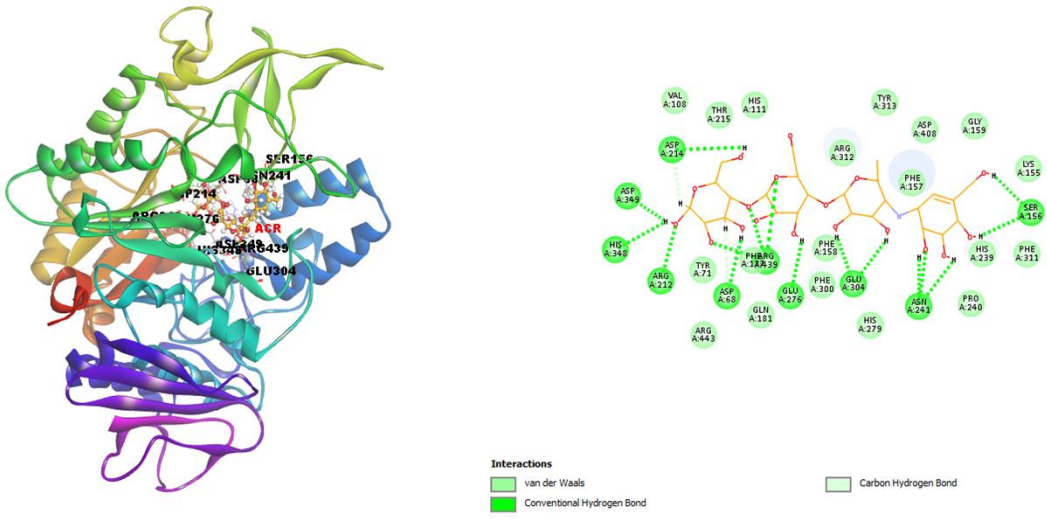

Figure S5. 3D and 2D docking poses and interactions of acarbose in the homology model of yeast alpha glucosidase (model 3).

Table S2. Interaction types and distances of **1d, 2c** and *Tacrine (TAC) compounds against AChE; **1c, 2c** and *Tacrin (TAC) compounds against BChE; **2a, 2d** and *Acarbose (ACR) compounds against α-Amy and **2a, 2d** and *Acarbose (ACR) compounds against α-Gly. The (*) mark indicates positive compounds of respective targets.

Interactions (hAChE)	**Distance Å**	**Bonding**	**Bonding Types**	**Binding site of target (hAChE)**	**Binding site of ligand (1d)**
A:ARG296:HN - :1d:O21	2.6589	Hydrogen Bond	Conventional Hydrogen Bond	A:ARG296:HN	:1d:O21
:1d:H34 - A:TYR341:O	1.8545	Hydrogen Bond	Conventional Hydrogen Bond	A:TYR341:O	:1d:H34
:1d:H8 - A:TYR337:OH	2.2266	Hydrogen Bond	Conventional Hydrogen Bond	A:TYR337:OH	:1d:H8
:1d:N5 - A:TYR341	4.9855	Electrostatic	Pi-Cation	A:TYR341	:1d:N5
:1d:H20 - A:TRP286	2.8476	Hydrophobic	Pi-Sigma	A:TRP286	:1d:H20
:1d:S19 - A:PHE338	5.9157	Other	Pi-Sulfur	A:PHE338	:1d:S19
A:TRP286 - :1d	5.2246	Hydrophobic	Pi-Pi Stacked	A:TRP286	:1d
A:TRP286 - :1d	4.0409	Hydrophobic	Pi-Pi Stacked	A:TRP286	:1d
:1d:C42 - A:LEU289	4.7763	Hydrophobic	Alkyl	A:LEU289	:1d:C42
A:TRP286 - :1d:C42	5.0362	Hydrophobic	Pi-Alkyl	A:TRP286	:1d:C42
A:TRP286 - :1d:C46	4.0117	Hydrophobic	Pi-Alkyl	A:TRP286	:1d:C46
Interactions (hAChE)	**Distance Å**	**Bonding**	**Bonding Types**	**Binding site of target (hAChE)**	**Binding site of ligand (2c)**
A:GLY120:HN - :2c:O24	2.7093	Hydrogen Bond	Conventional Hydrogen Bond	A:GLY120:HN	:2c:O24
A:GLY121:HN - :2c:O23	2.2188	Hydrogen Bond	Conventional Hydrogen Bond	A:GLY121:HN	:2c:O23
A:GLY126:HN - :2c:O15	2.8364	Hydrogen Bond	Conventional Hydrogen Bond	A:GLY126:HN	:2c:O15
A:TYR133:HH - :2c:O24	2.2594	Hydrogen Bond	Conventional Hydrogen Bond	A:TYR133:HH	:2c:O24
A:SER203:HG - :2c:O23	2.9305	Hydrogen Bond	Conventional Hydrogen Bond	A:SER203:HG	:2c:O23
:2c:H37 - A:GLU202:OE1	2.1276	Hydrogen Bond	Conventional Hydrogen Bond	A:GLU202:OE1	:2c:H37
A:GLY120:HA1 - :2c:O23	2.2252	Hydrogen Bond	Carbon Hydrogen Bond	A:GLY120:HA1	:2c:O23
A:GLY126:HA2 - :2c:O15	2.5275	Hydrogen Bond	Carbon Hydrogen Bond	A:GLY126:HA2	:2c:O15
A:SER203:HB1 - :2c:O23	2.1507	Hydrogen Bond	Carbon Hydrogen Bond	A:SER203:HB1	:2c:O23
A:GLY448:HA1 - :2c:N45	2.5325	Hydrogen Bond	Carbon Hydrogen Bond	A:GLY448:HA1	:2c:N45
:2c:H14 - A:TYR337	2.3771	Hydrophobic	Pi-Sigma	A:TYR337	:2c:H14
A:TRP86 - :2c	4.9761	Hydrophobic	Pi-Pi T-shaped	A:TRP86	:2c
A:TRP86 - :2c	4.7236	Hydrophobic	Pi-Pi T-shaped	A:TRP86	:2c
A:TYR337 - :2c	4.7022	Hydrophobic	Pi-Pi T-shaped	A:TYR337	:2c
A:TYR337 - :2c	4.8115	Hydrophobic	Pi-Pi T-shaped	A:TYR337	:2c
A:TYR341 - :2c	4.5476	Hydrophobic	Pi-Pi T-shaped	A:TYR341	:2c

A:GLY120:C,O;GLY121:N - :2c	3.6875	Hydrophobic	Amide-Pi Stacked	A:GLY120:C,O;GLY121:N	:2c
A:TRP86 - :2c:C46	3.8015	Hydrophobic	Pi-Alkyl	A:TRP86	:2c:C46
A:TRP86 - :2c:C46	4.0886	Hydrophobic	Pi-Alkyl	A:TRP86	:2c:C46
A:TYR337 - :2c:C46	4.1056	Hydrophobic	Pi-Alkyl	A:TYR337	:2c:C46
A:TYR449 - :2c:C46	4.2911	Hydrophobic	Pi-Alkyl	A:TYR449	:2c:C46
Interactions (hAChE)	**Distance Å**	**Bonding**	**Bonding Types**	**Binding site of target (hAChE)**	**Binding site of ligand (TAC)**
:TAC:H27 - A:GLU202:OE1	1.9707	Hydrogen Bond	Conventional Hydrogen Bond	A:GLU202:OE1	:TAC:H27
A:TRP86 - :TAC	4.09792	Hydrophobic	Pi-Pi Stacked	A:TRP86	:TAC
A:TRP86 - :TAC	4.9289	Hydrophobic	Pi-Pi Stacked	A:TRP86	:TAC
A:TRP86 - :TAC	3.7454	Hydrophobic	Pi-Pi Stacked	A:TRP86	:TAC
A:TRP86 - :TAC	4.6813	Hydrophobic	Pi-Pi Stacked	A:TRP86	:TAC
A:TRP86 - :TAC	4.9323	Hydrophobic	Pi-Alkyl	A:TRP86	:TAC
A:TRP86 - :TAC	4.6616	Hydrophobic	Pi-Alkyl	A:TRP86	:TAC
A:TYR337 - :TAC	4.8422	Hydrophobic	Pi-Alkyl	A:TYR337	:TAC
A:HIS447 - :TAC	4.5681	Hydrophobic	Pi-Alkyl	A:HIS447	:TAC

Interactions (hBChE)	**Distance Å**	**Bonding**	**Bonding Types**	**Binding site of target (hBChE)**	**Binding site of ligand (1c)**
A:ASP70:HN - :1c:S8	3.0736	Hydrogen Bond	Conventional Hydrogen Bond	A:ASP70:HN	:1c:S8
A:GLY115:HN - :1c:O20	2.2901	Hydrogen Bond	Conventional Hydrogen Bond	A:GLY115:HN	:1c:O20
A:TYR128:HH - :1c:O20	2.5398	Hydrogen Bond	Conventional Hydrogen Bond	A:TYR128:HH	:1c:O20
:1c:H24 - A:TRP82:O	1.6675	Hydrogen Bond	Conventional Hydrogen Bond	A:TRP82:O	:1c:H24
:1c:H34 - A:GLU197:OE2	2.0978	Hydrogen Bond	Conventional Hydrogen Bond	A:GLU197:OE2	:1c:H34
A:GLY115:HA1 - :1c:O21	2.6060	Hydrogen Bond	Carbon Hydrogen Bond	A:GLY115:HA1	:1c:O21
A:SER198:HB1 - :1c:O21	2.4618	Hydrogen Bond	Carbon Hydrogen Bond	A:SER198:HB1	:1c:O21
:1c:H18 - A:HIS438:O	2.4106	Hydrogen Bond	Carbon Hydrogen Bond	A:HIS438:O	:1c:H18
A:HIS438:NE2 - :1c	4.1840	Electrostatic	Pi-Cation	A:HIS438:NE2	:1c
A:ASP70:OD2 - :1c	3.4519	Electrostatic	Pi-Anion	A:ASP70:OD2	:1c
A:TRP82:HB1 - :1c	2.9088	Hydrophobic	Pi-Sigma	A:TRP82:HB1	:1c
A:TRP82 - :1c	4.5388	Hydrophobic	Pi-Pi T-shaped	A:TRP82	:1c
A:TYR332 - :1c	5.2747	Hydrophobic	Pi-Pi T-shaped	A:TYR332	:1c
A:HIS438 - :1c	4.4959	Hydrophobic	Pi-Pi T-shaped	A:HIS438	:1c
A:GLY115:C,O;GLY116:N - :1c	3.9525	Hydrophobic	Amide-Pi Stacked	A:GLY115:C,O;GLY116:N	:1c

A:PHE329 - :1c:C43	4.9780	Hydrophobic	Pi-Alkyl	A:PHE329	:1c:C43
A:HIS438 - :1c:C43	4.6457	Hydrophobic	Pi-Alkyl	A:HIS438	:1c:C43
Interactions (hBChE)	**Distance Å**	**Bonding**	**Bonding Types**	**Binding site of target (hBChE)**	**Binding site of ligand (2c)**
A:GLY116:HN - :2c:O8	1.9683	Hydrogen Bond	Conventional Hydrogen Bond	A:GLY116:HN	:2c:O8
A:GLY117:HN - :2c:O8	2.0866	Hydrogen Bond	Conventional Hydrogen Bond	A:GLY117:HN	:2c:O8
A:ALA199:HN - :2c:O8	2.3976	Hydrogen Bond	Conventional Hydrogen Bond	A:ALA199:HN	:2c:O8
A:SER198:HB1 - :2c:O8	2.1835	Hydrogen Bond	Carbon Hydrogen Bond	A:SER198:HB1	:2c:O8
:2c:H13 - A:SER79:O	2.0776	Hydrogen Bond	Carbon Hydrogen Bond	A:SER79:O	:2c:H13
A:HIS438:NE2 - :2c	4.7794	Electrostatic	Pi-Cation	A:HIS438:NE2	:2c
A:ASP70:OD2 - :2c	2.8678	Electrostatic	Pi-Anion	A:ASP70:OD2	:2c
A:HIS438:HD2 - :2c	2.8974	Hydrophobic	Pi-Sigma	A:HIS438:HD2	:2c
:2c:H11 - A:TRP231	2.8851	Hydrophobic	Pi-Sigma	A:TRP231	:2c:H11
:2c:O15 - A:TRP82	2.7144	Other	Pi-Lone Pair	A:TRP82	:2c:O15
A:TRP231 - :2c	5.3616	Hydrophobic	Pi-Pi T-shaped	A:TRP231	:2c
A:TRP231 - :2c	5.3187	Hydrophobic	Pi-Pi T-shaped	A:TRP231	:2c
A:PHE329 - :2c	5.1296	Hydrophobic	Pi-Pi T-shaped	A:PHE329	:2c
A:HIS438 - :2c	5.1117	Hydrophobic	Pi-Pi T-shaped	A:HIS438	:2c
:2c - A:ALA328	5.0903	Hydrophobic	Pi-Alkyl	A:ALA328	:2c
:2c - A:LEU286	5.0752	Hydrophobic	Pi-Alkyl	A:LEU286	:2c
Interactions (hBChE)	**Distance Å**	**Bonding**	**Bonding Types**	**Binding site of target (hBChE)**	**Binding site of ligand (TAC)**
:TAC:H26 - A:TRP82:O	2.0179	Hydrogen Bond	Conventional Hydrogen Bond	A:TRP82:O	:TAC:H26
:TAC:H27 - A:GLN67:OE1	1.9669	Hydrogen Bond	Conventional Hydrogen Bond	A:GLN67:OE1	:TAC:H27
A:THR120:OG1 - :TAC	2.8443	Other	Pi-Lone Pair	A:THR120:OG1	:TAC
A:TRP82 - :TAC	5.3361	Hydrophobic	Pi-Alkyl	A:TRP82	:TAC
A:TRP82 - :TAC	5.0819	Hydrophobic	Pi-Alkyl	A:TRP82	:TAC

Interactions (α-Amy)	**Distance Å**	**Bonding**	**Bonding Types**	**Binding site of target (α-Amy)**	**Binding site of ligand (2a)**
A:ARG195:HH12 - :2a:O23	2.7789	Hydrogen Bond	Conventional Hydrogen Bond	A:ARG195:HH12	:2a:O23
:2a:H37 - A:ASP197:OD1	1.7643	Hydrogen Bond	Conventional Hydrogen Bond	A:ASP197:OD1	:2a:H37
:2a:H38 - A:GLU233:OE2	1.8153	Hydrogen Bond	Conventional Hydrogen Bond	A:GLU233:OE2	:2a:H38
A:HIS101:HE1 - :2a:O15	3.0949	Hydrogen Bond	Carbon Hydrogen Bond	A:HIS101:HE1	:2a:O15
:2a:S22 - A:TRP58	5.9748	Other	Pi-Sulfur	A:TRP58	:2a:S22

:2a:S22 - A:TYR62	4.0881	Other	Pi-Sulfur	A:TYR62	:2a:S22
:2a:S22 - A:HIS299	4.4537	Other	Pi-Sulfur	A:HIS299	:2a:S22
A:TRP59 - :2a	4.6373	Hydrophobic	Pi-Pi Stacked	A:TRP59	:2a
A:TYR62 - :2a	4.1764	Hydrophobic	Pi-Pi Stacked	A:TYR62	:2a
A:TRP58 - :2a	4.8265	Hydrophobic	Pi-Pi T-shaped	A:TRP58	:2a
Interactions (α-Amy)	**Distance Å**	**Bonding**	**Bonding Types**	**Binding site of target (α-Amy)**	**Binding site of ligand (2d)**
A:HIS101:HE2 - :2d:O23	2.0095	Hydrogen Bond	Conventional Hydrogen Bond	A:HIS101:HE2	:2d:O23
A:HIS201:HE2 - :2d:O15	1.9414	Hydrogen Bond	Conventional Hydrogen Bond	A:HIS201:HE2	:2d:O15
:2d:H37 - A:ASP197:OD2	1.8565	Hydrogen Bond	Conventional Hydrogen Bond	A:ASP197:OD2	:2d:H37
A:ASP300:OD1 - :2d	3.6214	Electrostatic	Pi-Anion	A:ASP300:OD1	:2d
A:TYR62 - :2d	4.0569	Hydrophobic	Pi-Pi Stacked	A:TYR62	:2d
A:TRP58 - :2d:C45	3.9258	Hydrophobic	Pi-Alkyl	A:TRP58	:2d:C45
A:TYR62 - :2d:C45	4.2632	Hydrophobic	Pi-Alkyl	A:TYR62	:2d:C45
A:HIS299 - :2d:C49	3.9176	Hydrophobic	Pi-Alkyl	A:HIS299	:2d:C49
:2d - A:LEU162	4.8026	Hydrophobic	Pi-Alkyl	A:LEU162	:2d
:2d - A:ALA198	4.4036	Hydrophobic	Pi-Alkyl	A:ALA198	:2d
:2d - A:ILE235	5.0145	Hydrophobic	Pi-Alkyl	A:ILE235	:2d
Interactions (α-Amy)	**Distance Å**	**Bonding**	**Bonding Types**	**Binding site of target (α-Amy)**	**Binding site of ligand (ACR)**
A:GLN63:HE22 - :ACR:O18	1.6702	Hydrogen Bond	Conventional Hydrogen Bond	A:GLN63:HE22	:ACR:O18
A:ASN298:HD21 - :ACR:O7	2.0254	Hydrogen Bond	Conventional Hydrogen Bond	A:ASN298:HD21	:ACR:O7
A:ASN301:HN - :ACR:O9	2.6100	Hydrogen Bond	Conventional Hydrogen Bond	A:ASN301:HN	:ACR:O9
:ACR:H77 - A:ASP300:OD2	2.9104	Hydrogen Bond	Conventional Hydrogen Bond	A:ASP300:OD2	:ACR:H77
:ACR:H87 - A:TRP59:O	1.7371	Hydrogen Bond	Conventional Hydrogen Bond	A:TRP59:O	:ACR:H87
:ACR:H70 - A:ASP197:OD1	2.2595	Hydrogen Bond	Conventional Hydrogen Bond	A:ASP197:OD1	:ACR:H70
:ACR:H72 - A:GLU233:OE2	1.9303	Hydrogen Bond	Conventional Hydrogen Bond	A:GLU233:OE2	:ACR:H72
:ACR:H73 - A:GLU233:OE2	1.7352	Hydrogen Bond	Conventional Hydrogen Bond	A:GLU233:OE2	:ACR:H73
:ACR:H74 - A:ASP300:OD1	2.2284	Hydrogen Bond	Conventional Hydrogen Bond	A:ASP300:OD1	:ACR:H74
:ACR:H81 - A:ASP300:OD1	1.6743	Hydrogen Bond	Conventional Hydrogen Bond	A:ASP300:OD1	:ACR:H81
:ACR:H86 - A:ASP300:OD1	2.5189	Hydrogen Bond	Conventional Hydrogen Bond	A:ASP300:OD1	:ACR:H86
A:ASN301:HA - :ACR:O17	1.9122	Hydrogen Bond	Carbon Hydrogen Bond	A:ASN301:HA	:ACR:O17
:ACR:H15 - A:GLU233:OE2	2.8086	Hydrogen Bond	Carbon Hydrogen Bond	A:GLU233:OE2	:ACR:H15
:ACR:H20 - A:GLU233:OE2	2.3565	Hydrogen Bond	Carbon Hydrogen Bond	A:GLU233:OE2	:ACR:H20

:ACR:H27 - A:ASP197:OD1	2.7183	Hydrogen Bond	Carbon Hydrogen Bond	A:ASP197:OD1	:ACR:H27
:ACR:H27 - A:GLU233:OE1	2.5169	Hydrogen Bond	Carbon Hydrogen Bond	A:GLU233:OE1	:ACR:H27
:ACR:H37 - A:ASP300:OD1	2.8195	Hydrogen Bond	Carbon Hydrogen Bond	A:ASP300:OD1	:ACR:H37
A:ALA198 - :ACR:C35	4.4052	Hydrophobic	Alkyl	A:ALA198	:ACR:C35
:ACR:C35 - A:LEU162	4.5427	Hydrophobic	Alkyl	A:LEU162	:ACR:C35
A:HIS201 - :ACR:C35	5.1708	Hydrophobic	Pi-Alkyl	A:HIS201	:ACR:C35

Interactions (α-Gly)	**Distance Å**	**Bonding**	**Bonding Types**	**Binding site of target (α-Gly)**	**Binding site of ligand (2a)**
A:ARG312:HE - :2a:O23	1.7950	Hydrogen Bond	Conventional Hydrogen Bond	A:ARG312:HE	:2a:O23
A:TYR313:HH - :2a:O23	2.0359	Hydrogen Bond	Conventional Hydrogen Bond	A:TYR313:HH	:2a:O23
A:ASN412:HD22 - :2a:O15	1.9822	Hydrogen Bond	Conventional Hydrogen Bond	A:ASN412:HD22	:2a:O15
:2a:H38 - A:ASP408:OD1	2.1588	Hydrogen Bond	Conventional Hydrogen Bond	A:ASP408:OD1	:2a:H38
A:HIS239:HE1 - :2a:O8	1.8895	Hydrogen Bond	Carbon Hydrogen Bond	A:HIS239:HE1	:2a:O8
A:PHE311:HA - :2a:O8	2.3282	Hydrogen Bond	Carbon Hydrogen Bond	A:PHE311:HA	:2a:O8
:2a:S14 - A:PHE311	4.6604	Other	Pi-Sulfur	A:PHE311	:2a:S14
:2a:S22 - A:TYR313	5.4500	Other	Pi-Sulfur	A:TYR313	:2a:S22
:2a - A:ARG312	3.8643	Hydrophobic	Pi-Alkyl	A:ARG312	:2a
:2a - A:ARG312	4.8447	Hydrophobic	Pi-Alkyl	A:ARG312	:2a
Interactions (α-Gly)	**Distance Å**	**Bonding**	**Bonding Types**	**Binding site of target (α-Gly)**	**Binding site of ligand (2d)**
A:ASN241:HD22 - :2d:S14	2.3887	Hydrogen Bond	Conventional Hydrogen Bond	A:ASN241:HD22	:2d:S14
A:ARG439:HH11 - :2d:O23	2.4599	Hydrogen Bond	Conventional Hydrogen Bond	A:ARG439:HH11	:2d:O23
A:ARG439:HH11 - :2d:N44	2.7297	Hydrogen Bond	Conventional Hydrogen Bond	A:ARG439:HH11	:2d:N44
:2d:H37 - A:GLU276:OE2	1.9451	Hydrogen Bond	Conventional Hydrogen Bond	A:GLU276:OE2	:2d:H37
A:ARG439:HD2 - :2d:O23	2.9097	Hydrogen Bond	Carbon Hydrogen Bond	A:ARG439:HD2	:2d:O23
:2d:S14 - A:ASN241:OD1	3.1329	Other	Sulfur-X	A:ASN241:OD1	:2d:S14
:2d:S14 - A:ASN241:ND2	3.2850	Other	Sulfur-X	A:ASN241:ND2	:2d:S14
A:ASP214:OD1 - :2d	3.7694	Electrostatic	Pi-Anion	A:ASP214:OD1	:2d
:2d:H15 - A:PHE177	2.3103	Hydrophobic	Pi-Sigma	A:PHE177	:2d:H15
:2d:S14 - A:HIS279	5.2535	Other	Pi-Sulfur	A:HIS279	:2d:S14
A:PHE300 - :2d	4.7758	Hydrophobic	Pi-Pi T-shaped	A:PHE300	:2d
A:TYR71 - :2d:C45	3.6057	Hydrophobic	Pi-Alkyl	A:TYR71	:2d:C45
A:HIS111 - :2d:C49	4.2511	Hydrophobic	Pi-Alkyl	A:HIS111	:2d:C49

A:HIS348 - :2d:C45	4.4027	Hydrophobic	Pi-Alkyl	A:HIS348	:2d:C45
:2d - A:ARG312	4.0951	Hydrophobic	Pi-Alkyl	A:ARG312	:2d
Interactions (α-Gly)	**Distance Å**	**Bonding**	**Bonding Types**	**Binding site of target (α-Gly)**	**Binding site of ligand (ACR)**
A:ARG212:HH12 - :ACR:O16	2.7103	Hydrogen Bond	Conventional Hydrogen Bond	A:ARG212:HH12	:ACR:O16
A:ARG212:HH22 - :ACR:O16	2.1753	Hydrogen Bond	Conventional Hydrogen Bond	A:ARG212:HH22	:ACR:O16
A:ASN241:HD22 - :ACR:O10	2.1833	Hydrogen Bond	Conventional Hydrogen Bond	A:ASN241:HD22	:ACR:O10
A:ARG439:HH11 - :ACR:O3	1.8509	Hydrogen Bond	Conventional Hydrogen Bond	A:ARG439:HH11	:ACR:O3
A:ARG439:HH11 - :ACR:O15	2.2442	Hydrogen Bond	Conventional Hydrogen Bond	A:ARG439:HH11	:ACR:O15
A:ARG439:HH12 - :ACR:O4	2.3330	Hydrogen Bond	Conventional Hydrogen Bond	A:ARG439:HH12	:ACR:O4
:ACR:H77 - A:ASN241:OD1	2.0611	Hydrogen Bond	Conventional Hydrogen Bond	A:ASN241:OD1	:ACR:H77
:ACR:H80 - A:ASN241:OD1	2.2174	Hydrogen Bond	Conventional Hydrogen Bond	A:ASN241:OD1	:ACR:H80
:ACR:H82 - A:SER156:O	2.2023	Hydrogen Bond	Conventional Hydrogen Bond	A:SER156:O	:ACR:H82
:ACR:H87 - A:SER156:O	1.9009	Hydrogen Bond	Conventional Hydrogen Bond	A:SER156:O	:ACR:H87
:ACR:H70 - A:GLU304:OE2	1.9899	Hydrogen Bond	Conventional Hydrogen Bond	A:GLU304:OE2	:ACR:H70
:ACR:H72 - A:GLU304:OE2	1.7773	Hydrogen Bond	Conventional Hydrogen Bond	A:GLU304:OE2	:ACR:H72
:ACR:H73 - A:GLU276:OE2	2.1563	Hydrogen Bond	Conventional Hydrogen Bond	A:GLU276:OE2	:ACR:H73
:ACR:H81 - A:ASP68:OD2	2.4232	Hydrogen Bond	Conventional Hydrogen Bond	A:ASP68:OD2	:ACR:H81
:ACR:H85 - A:HIS348:NE2	2.3192	Hydrogen Bond	Conventional Hydrogen Bond	A:HIS348:NE2	:ACR:H85
:ACR:H85 - A:ASP349:OD2	1.9445	Hydrogen Bond	Conventional Hydrogen Bond	A:ASP349:OD2	:ACR:H85
:ACR:H86 - A:ASP214:OD2	2.0583	Hydrogen Bond	Conventional Hydrogen Bond	A:ASP214:OD2	:ACR:H86
:ACR:H38 - A:ASP68:OD2	2.3359	Hydrogen Bond	Carbon Hydrogen Bond	A:ASP68:OD2	:ACR:H38
:ACR:H40 - A:ASP214:OD1	1.8479	Hydrogen Bond	Carbon Hydrogen Bond	A:ASP214:OD1	:ACR:H40

1a

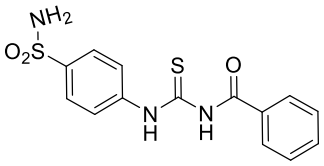

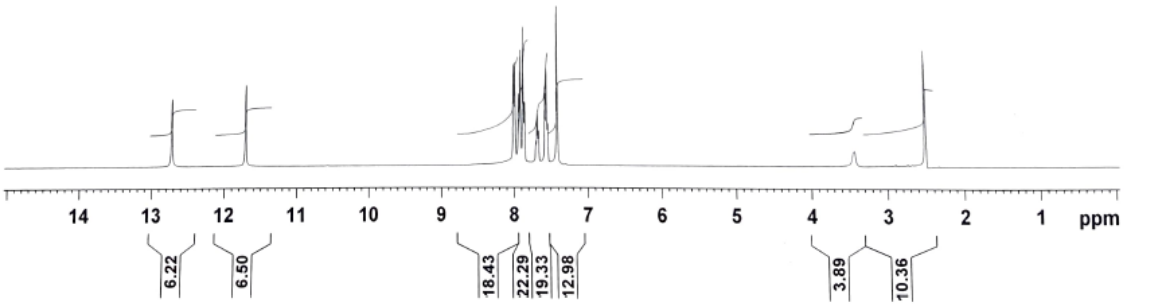

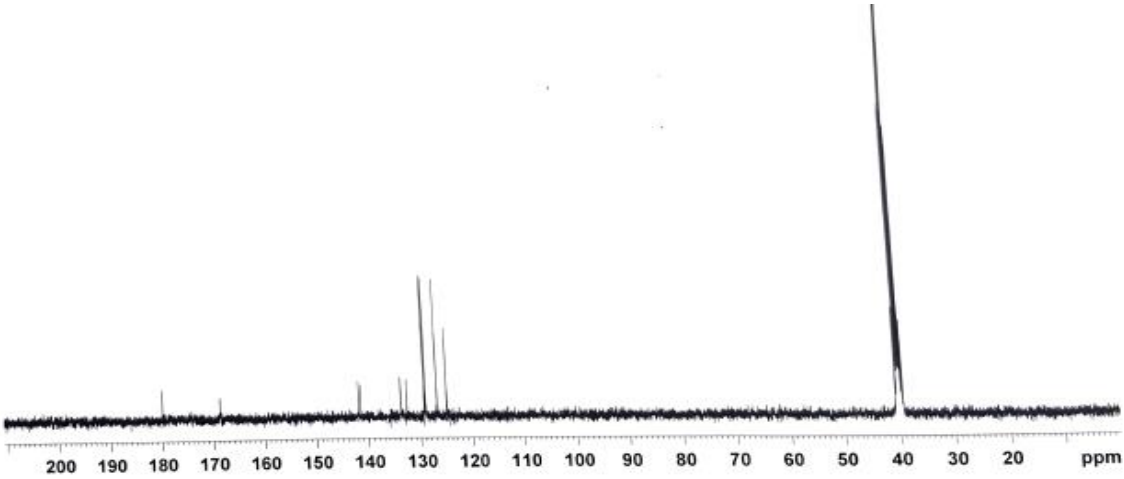

C14 H13 N3 O3 S2 [M-H]- : Predicted region for 334.0326 m/z

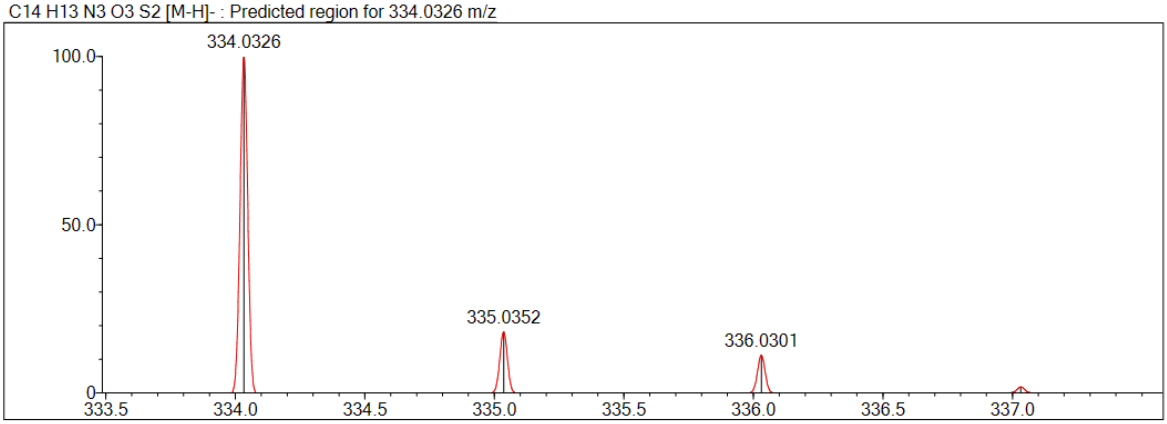

Rank	Score	Formula (M)	Ion	Meas. m/z	Pred. m/z	Df. (mDa)	Df. (ppm)	Iso	DBE
1	29.90	C14 H13 N3 O3 S2	[M-H]-	334.0330	334.0326	0.4	1.20	30.05	10.0

1b

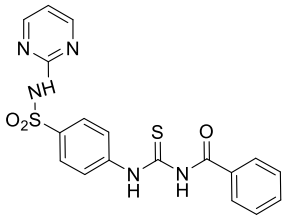

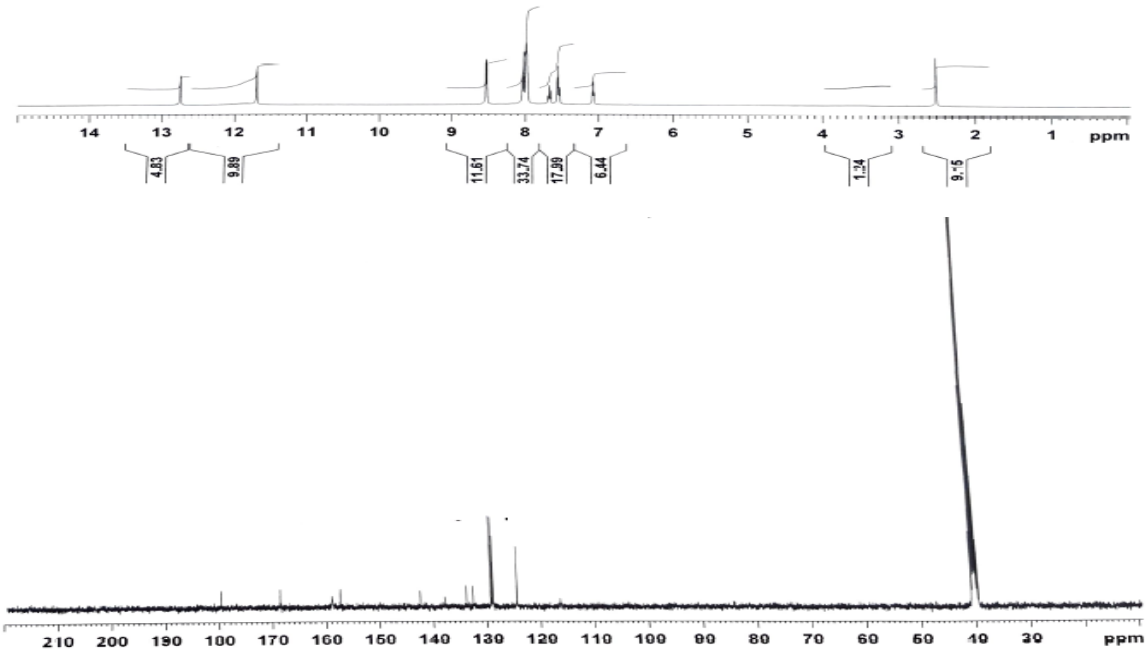

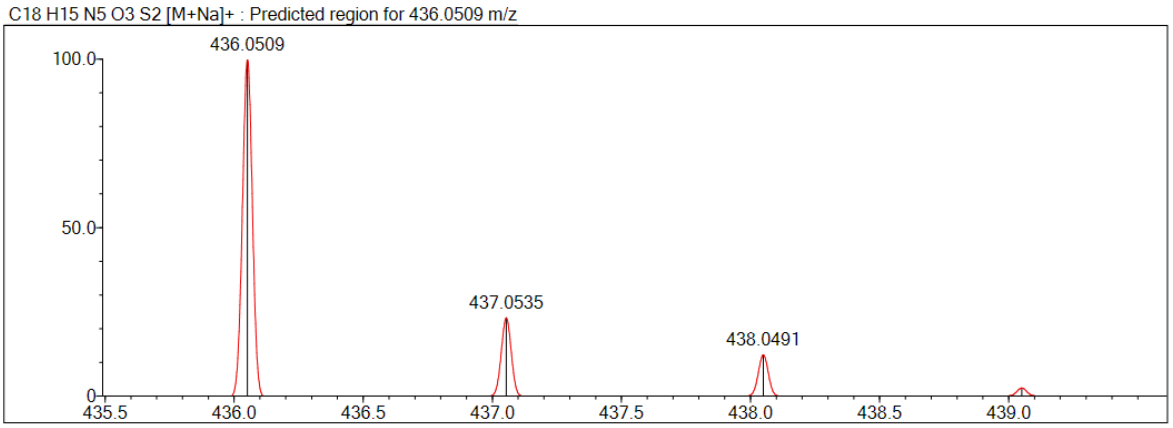

Rank	Score	Formula (M)	Ion	Meas. m/z	Pred. m/z	Df. (mDa)	Df. (ppm)	Iso	DBE
1	68.24	C18 H15 N5 O3 S2	[M+Na]+	436.0502	436.0509	-0.7	-1.61	69.30	14.0

1c

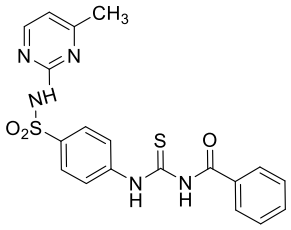

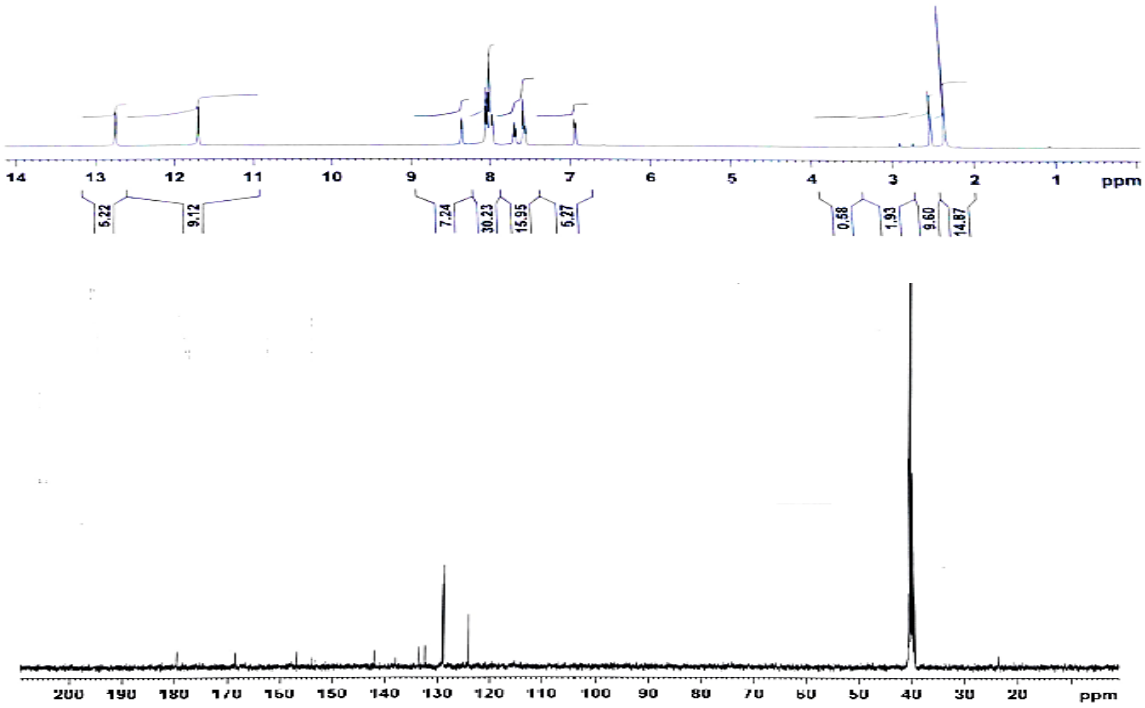

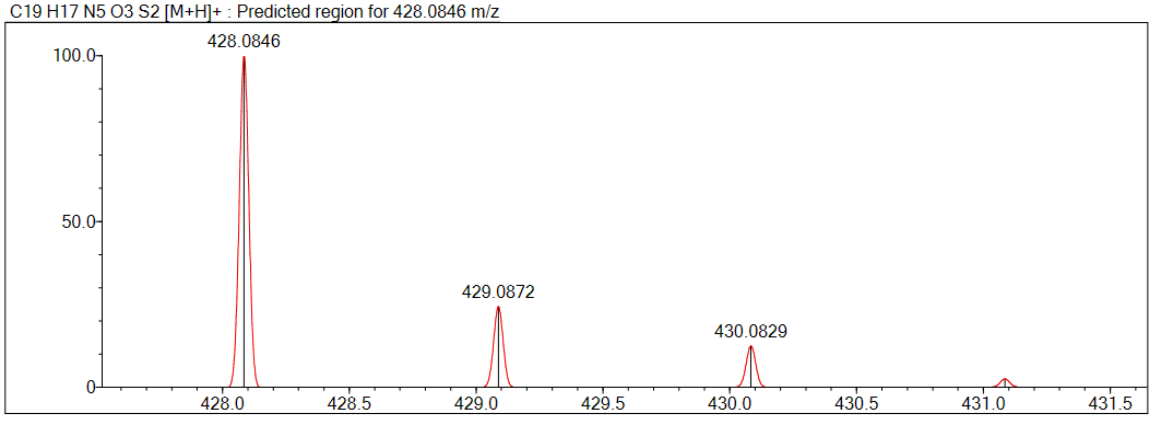

Rank	Score	Formula (M)	Ion	Meas. m/z	Pred. m/z	Df. (mDa)	Df. (ppm)	Iso	DBE
1	37.19	C19 H17 N5 O3 S2	[M+H]+	428.0834	428.0846	-1.2	-2.80	38.94	14.0

1d

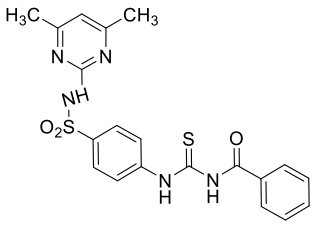

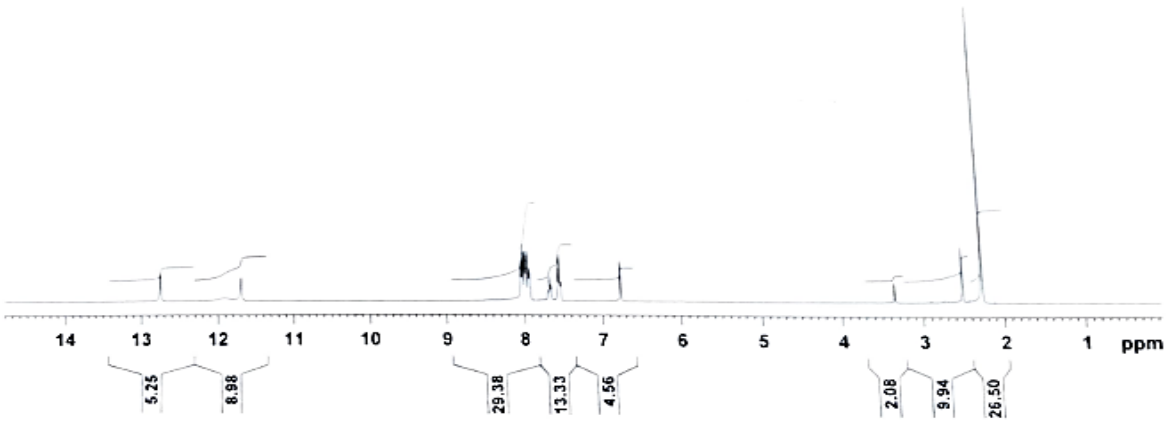

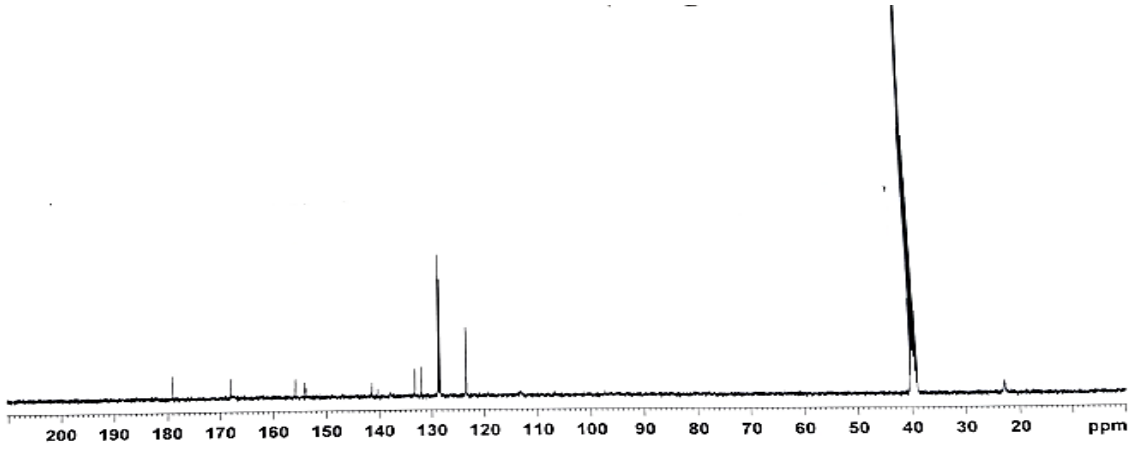

C20 H19 N5 O3 S2 [M+H]+ : Predicted region for 442.1002 m/z

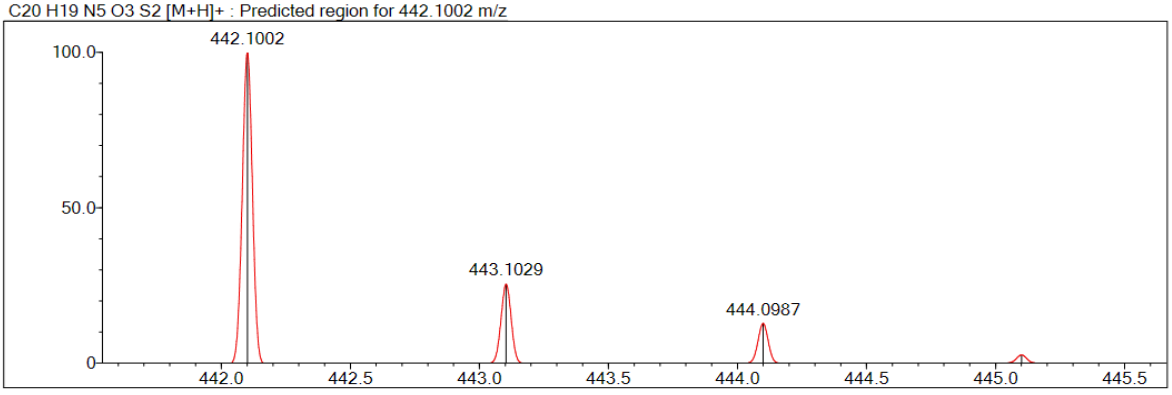

Rank	Score	Formula (M)	Ion	Meas. m/z	Pred. m/z	Df. (mDa)	Df. (ppm)	Iso	DBE
1	63.26	C20 H19 N5 O3 S2	[M+H]+	442.1006	442.1002	0.4	0.90	63.26	14.0

2a

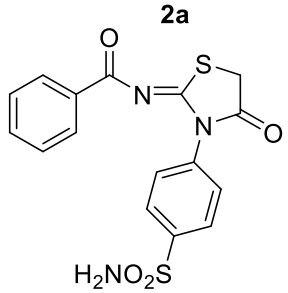
O
S
N
N
O
H_2NO_2S

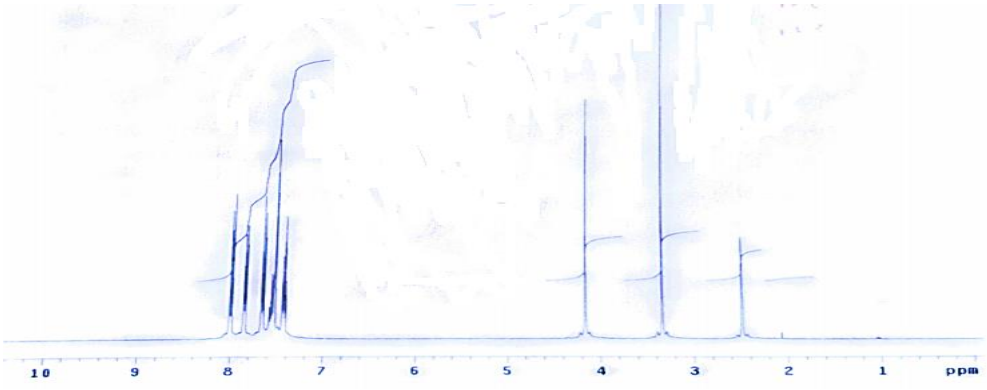
10
9
8
7
6
5
4
3
2
1
ppm

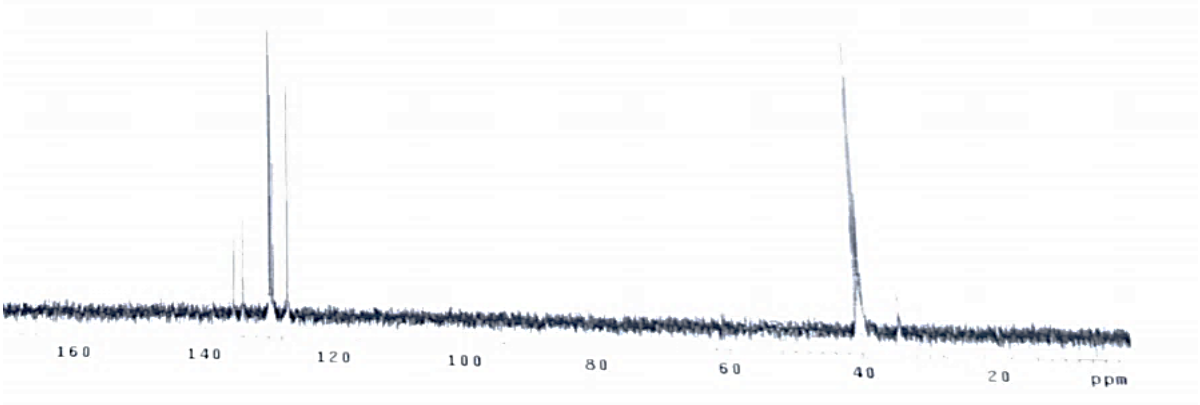
160
140
120
100
80
60
40
20
ppm

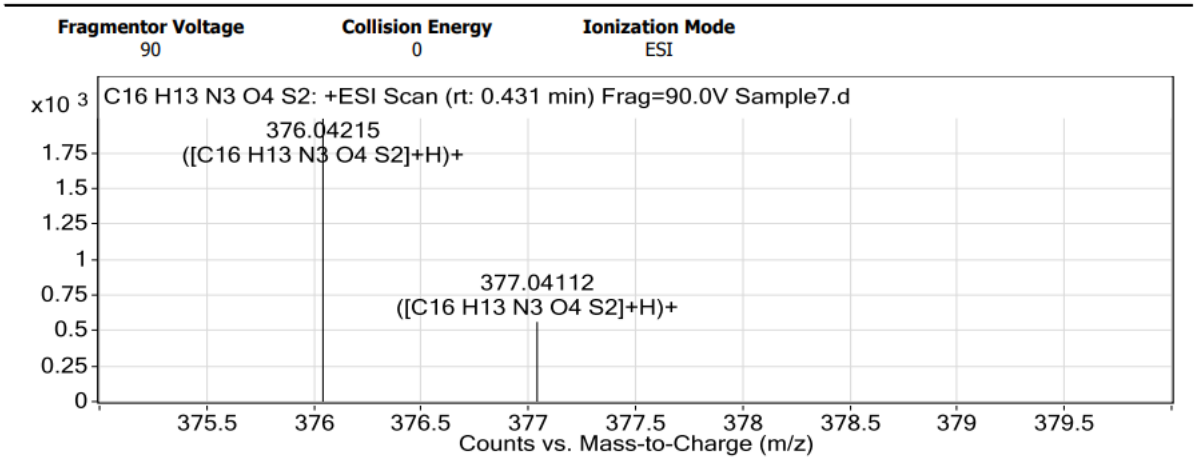
Fragmentor Voltage
90
Collision Energy
0
Ionization Mode
ESI
x10 3
C16 H13 N3 O4 S2: +ESI Scan (rt: 0.431 min) Frag=90.0V Sample7.d
376.04215
([C16 H13 N3 O4 S2]+H)+
377.04112
([C16 H13 N3 O4 S2]+H)+
1.75
1.5
1.25
1
0.75
0.5
0.25
0
375.5
376
376.5
377
377.5
378
378.5
379
379.5
Counts vs. Mass-to-Charge (m/z)

2c

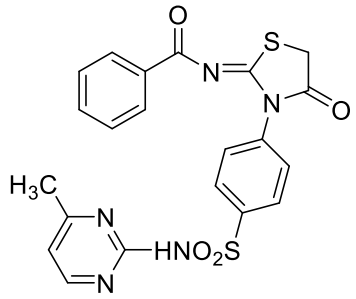

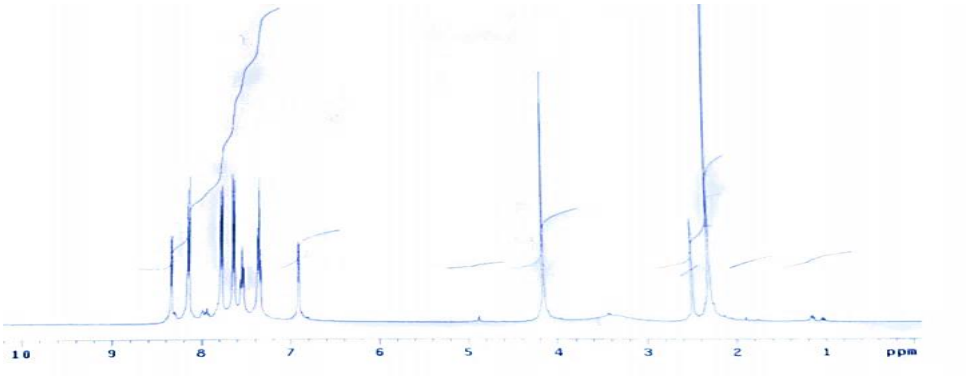

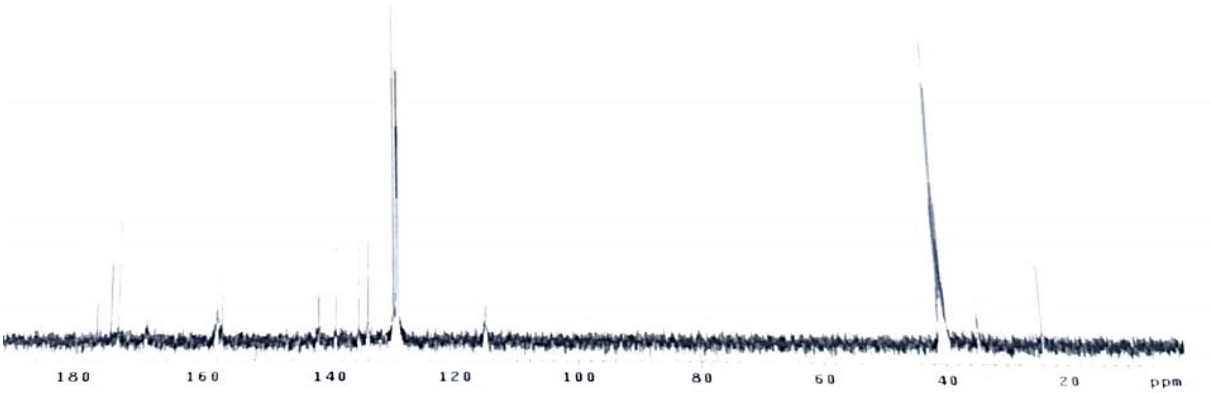

Fragmentor Voltage	Collision Energy	Ionization Mode
90	0	ESI

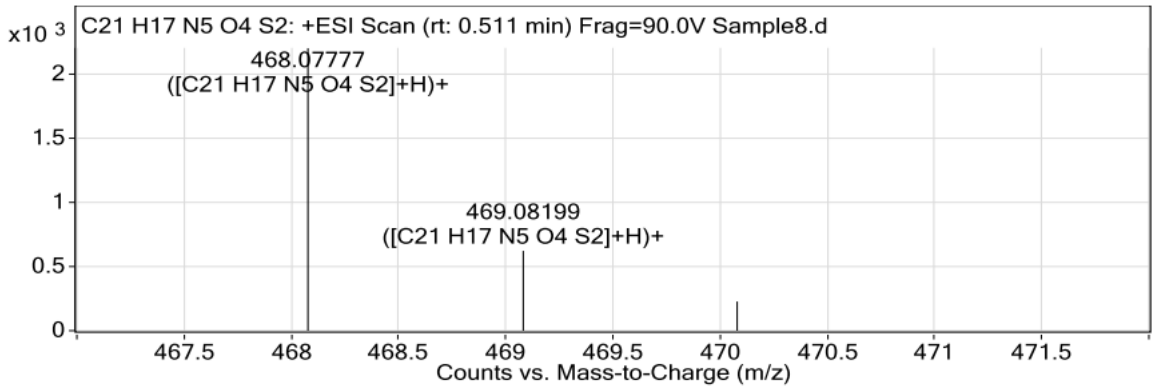

2d

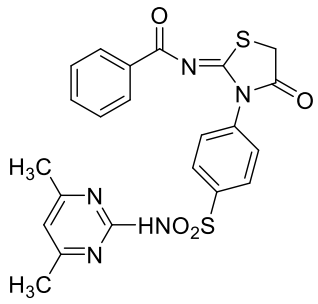

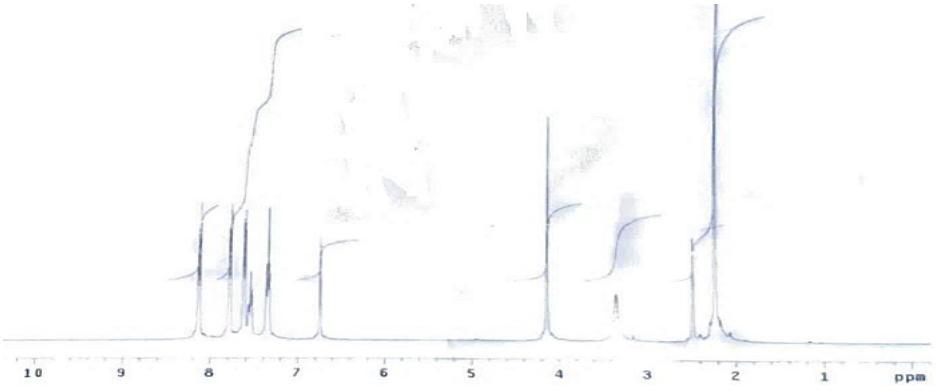

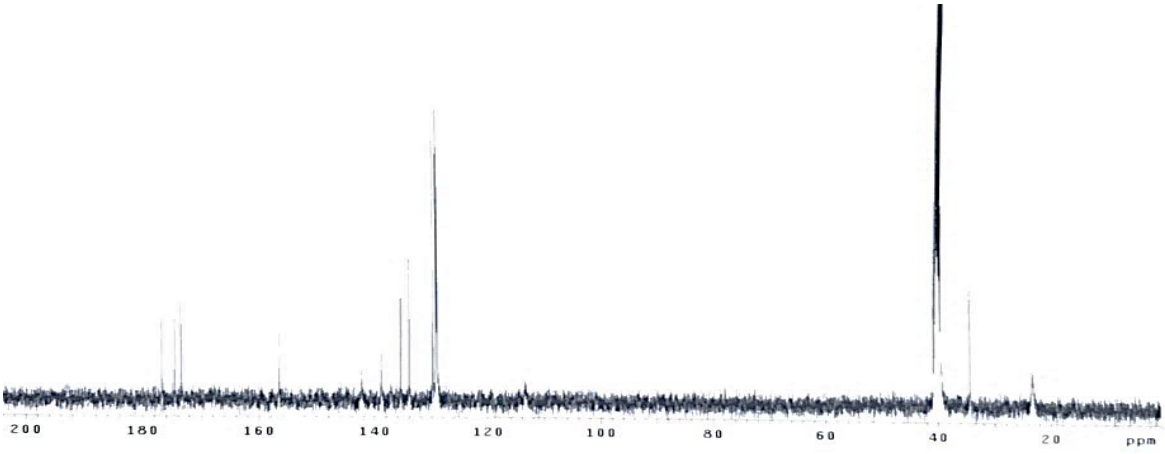

-

Fragmentor Voltage	Collision Energy	Ionization Mode
90	0	ESI